

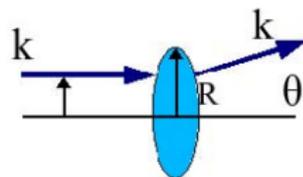
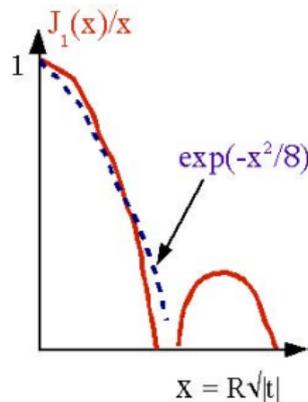
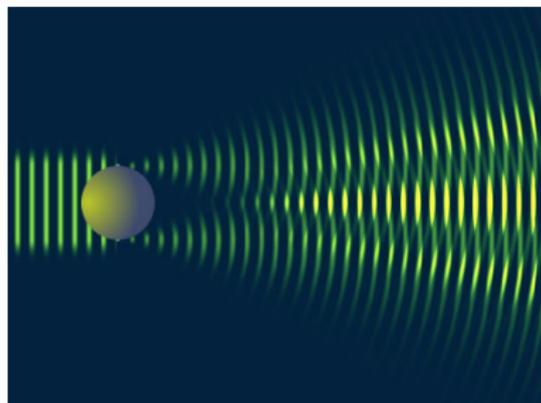
Measurement of the cross-section ratio $\sigma_{\psi(2S)}/\sigma_{J/\psi(1S)}$ in exclusive photoproduction at HERA

Grzegorz Grzelak

Faculty of Physics
University of Warsaw



High Energy Physics Seminar, Warsaw, May 27th 2022

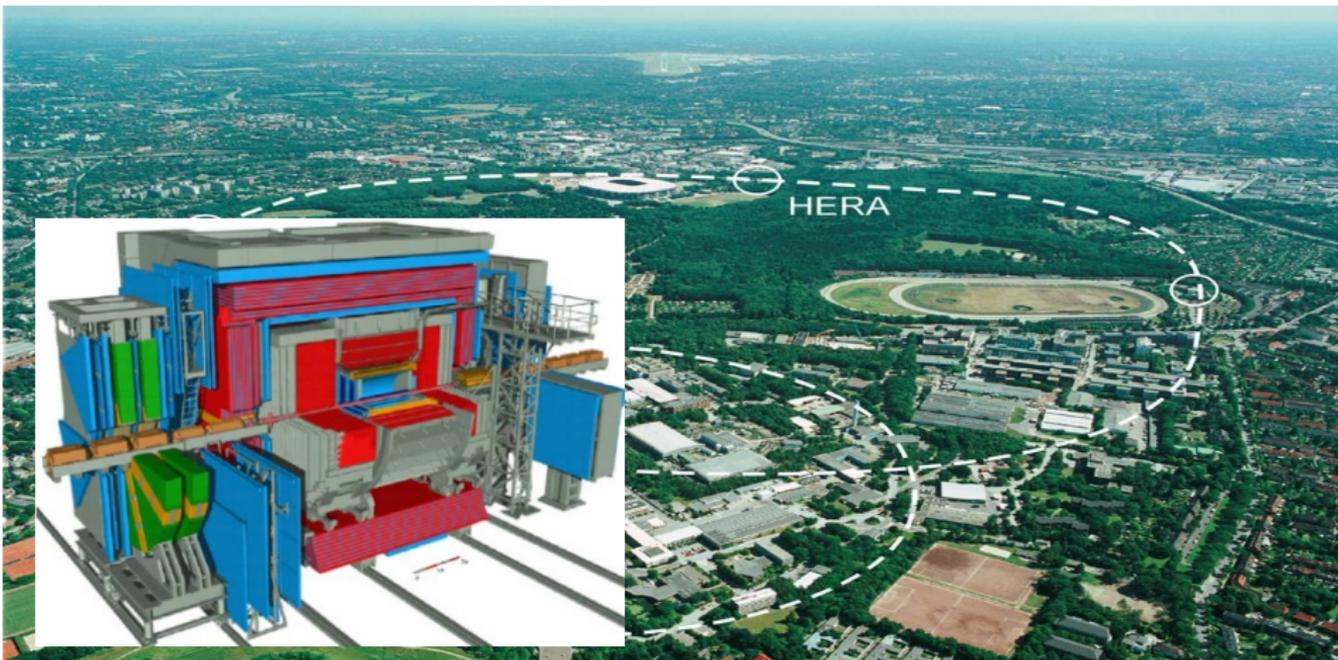


Light Scattering in Fraunhofer approximation (wavelength $\lambda \sim 1/k \ll R$)

- $|t| = 4k^2 \sin^2(\theta/2)$
- $d\sigma/dt \sim e^{-b|t|}$ (first diffractive peak approximated from Bessel function)
- $b = (R/2)^2 \rightarrow$ transverse size of the target
- in the presented studies: **target \equiv proton** and **photon energy $\gg 1$ GeV**

HERA and ZEUS: 1992 – 2007, DESY, Hamburg

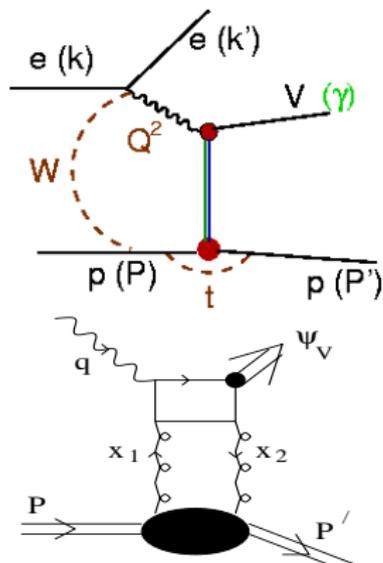
HERA: world's first and only $e^\pm p$ collider, $E_e = 27.5 \text{ GeV}$, $E_p = 920 \text{ GeV}$ ($\sqrt{s} = 318 \text{ GeV}$)



ZEUS: multipurpose, hermetic detector (MVD, CTD, CAL, F/B/RMUON, BAC, ...)

Total luminosity: $\int \mathcal{L} \sim 500 \text{ pb}^{-1}$ collected during HERA I + II running periods

Production of Vector Mesons in Exclusive Diffraction in ep Scattering



Exclusive process: proton stays intact
 Proton dissociation also possible \rightarrow
 background

pQCD: M_V^2 and Q^2 - set the scale at which the W and $|t|$ are probed
 Process sensitive to the **gluon density** in the proton

Kinematics: $M_V^2, Q^2, W, |t|$

M_V^2 - vector meson mass squared

$Q^2 (= -q^2 = -(k - k')^2)$ - the photon virtuality
 (emitted by the incoming electron):

- $Q^2 \approx 0$ GeV² PHP (*Photoproduction*)
- larger Q^2 for DIS (*Deep Inelastic Scattering*)

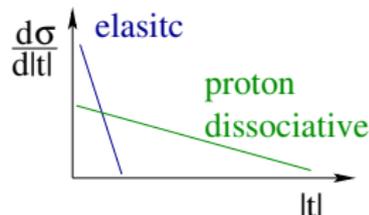
$W = (q + P)^2$ - invariant mass of the γp system

$$W \approx \sqrt{2E_P(E - p_Z)}_V$$

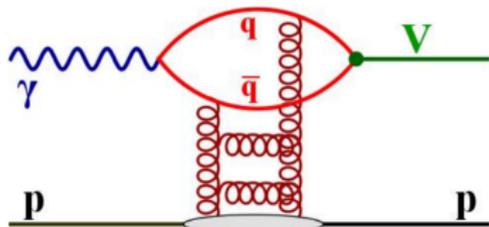
$|t|$ - 4-momentum transfer at the proton vertex

$$t = (P - P')^2$$

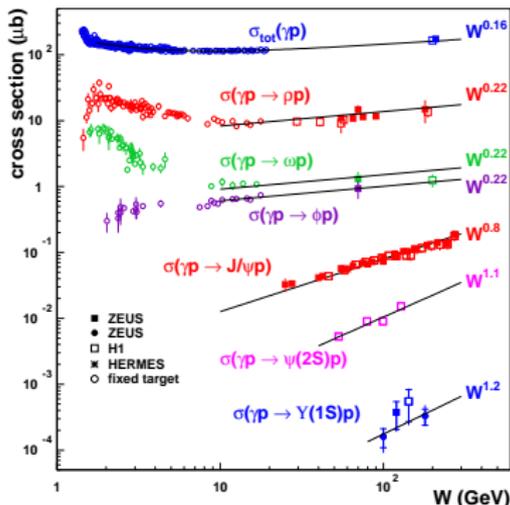
$$t \approx -p_{T,V}^2$$

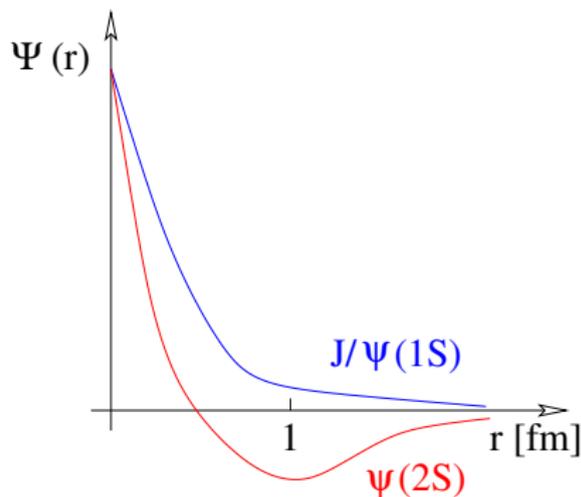


W-dependence of the VM exclusive cross section for PHP: $\sigma(\gamma p \rightarrow Vp)$



- process driven by gluons
 - $\sigma \propto [xg(x, \mu^2)]^2$
 - $x = \mu^2/W^2$: high $W \rightarrow$ small x
 - $\mu^2 \propto (Q^2 + M_V^2)$
-
- total cross sections σ_{VM} for VM photoproduction spans over 6 orders of magnitude ! (for higher VM masses \rightarrow smaller transverse size of $q\bar{q} \rightarrow$ "color screening")
 - σ_{VM} rises with γp c.m. energy W as W^δ ($x \sim 1/W^2$: high $W \rightarrow$ small x) (for heavy VMs expected from the gluon behaviour in the proton \rightarrow probing small x)
 - power δ rises with M_V^2 from "soft" ($\delta \approx 0.22$) to "hard" ($\delta \approx 1.2$) processes



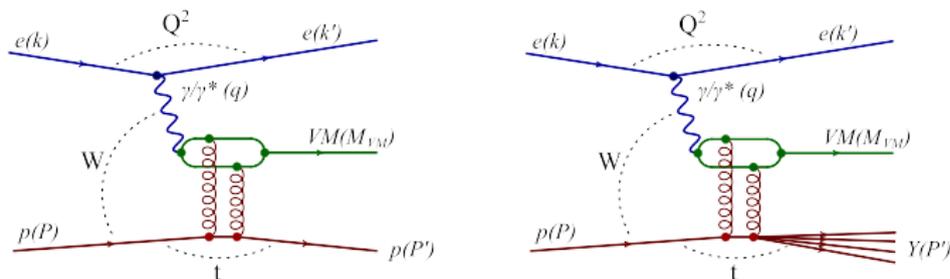


$$\text{Ratio } R = \frac{\sigma_{\gamma p \rightarrow \psi(2S)p}}{\sigma_{\gamma p \rightarrow J/\psi(1S)p}}$$

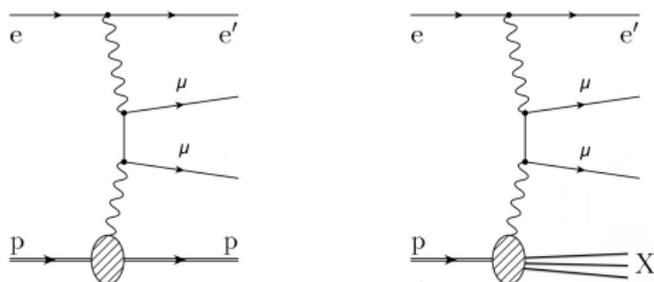
- sensitive to radial wave function of charmonium
- provides insight into the dynamics of the hard process
- (some systematics cancel out)

- $J/\psi(1S)$ and $\psi(2S)$ have the same quark composition but distinctive wave functions
- $\psi(2S)$ has a node at ≈ 0.4 fm
- $\langle r_{\psi(2S)}^2 \rangle \approx 2 \langle r_{J/\psi(1S)}^2 \rangle$
- pQCD models predict $R \sim 0.17$ in PHP and **rise of R with Q^2 in DIS**
- $\psi(2S)$ cross section is expected to be suppressed w.r.t. the J/ψ production
- (Both Vector Mesons masses are much smaller than the γp center-of-mass energy)

- **Signal MC: DIFFVM (VM production in ep scattering)**

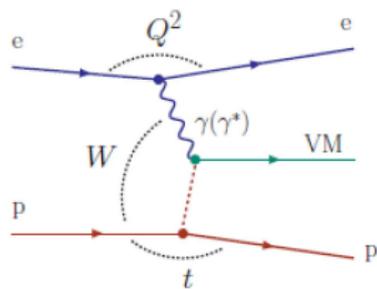
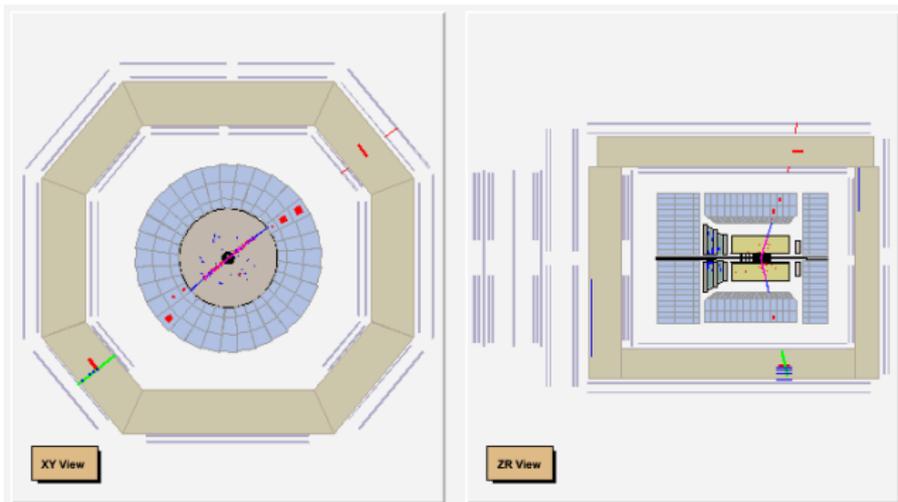


- **Background MC: GRAPE (Bethe-Heitler continuum $\mu^+\mu^-$)**



- **HERA II DATA:** $\mathcal{L} = 373 \text{ pb}^{-1}$ (2003 - 2007)
- **Investigated decay channels:**
 - $\psi(2S) \rightarrow \mu^+ \mu^-$, $\psi(2S) \rightarrow J/\psi + \pi^+ \pi^-$, $J/\psi(1S) \rightarrow \mu^+ \mu^-$
- **exclusive (elastic) photoproduction sample**
- **kinematic range (analysis phase space):**
 - $30 < W < 180 \text{ GeV}$
 - $|t| < 1.0 \text{ GeV}^2$
 - $Q^2 < 1 \text{ GeV}^2$ (median $Q^2 \approx 3 \times 10^{-5} \text{ GeV}^2$)

Example of Final State Topology for $ep \rightarrow J/\psi p$, $J/\psi \rightarrow \mu^+ \mu^-$



Exclusive process, reaction mediated by exchange of **colorless** object; **proton stays intact.**

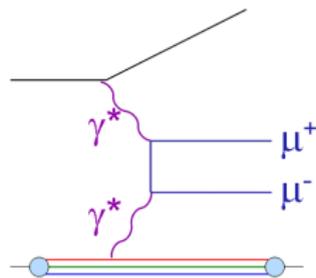
J/ψ and $\psi(2S)$ are detected in the 2- or 4-prong final states ($\mu^+ \mu^-$ or $\mu^+ \mu^- \pi^+ \pi^-$)
very clean final state topology:

Photoproduction ($Q^2 < 1 \text{ GeV}^2$): two or four charged particles and nothing else
 \implies **experimental challenge: triggering on soft muons**

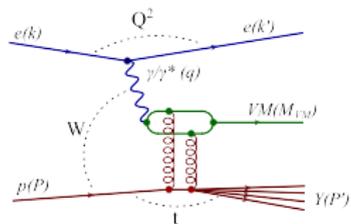
(Electroproduction ($Q^2 > 1 \text{ GeV}^2$): scattered electron also visible in the detector)

(NOTE THE OPENING ANGLE OF THE DECAY PRODUCTS !)

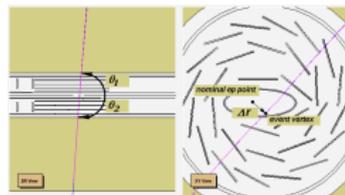
- QED di-muons (like $\gamma^* \gamma^* \rightarrow \mu^+ \mu^-$) from the Bethe-Heitler process



- J/ψ and $\psi(2S)$ mesons production with the dissociation of the proton



- Cosmic muons can mimic $\mu^+ \mu^-$ pairs when passing close to the interaction point

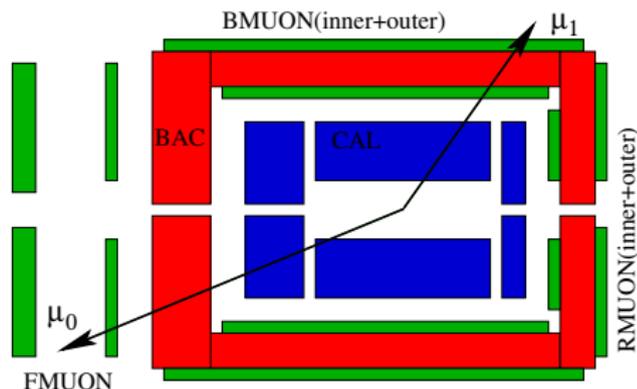


- **Muon efficiency corrections**

Single muon efficiency corrections: TAG and PROBE

- TAG: “the triggering” muon
- PROBE: “the tested” muon
- effic in given $(p_{t_{eff}}^j, \eta^j)$ bin:

$$\epsilon = N_{PROBE}^j / N_{TAG}^i$$



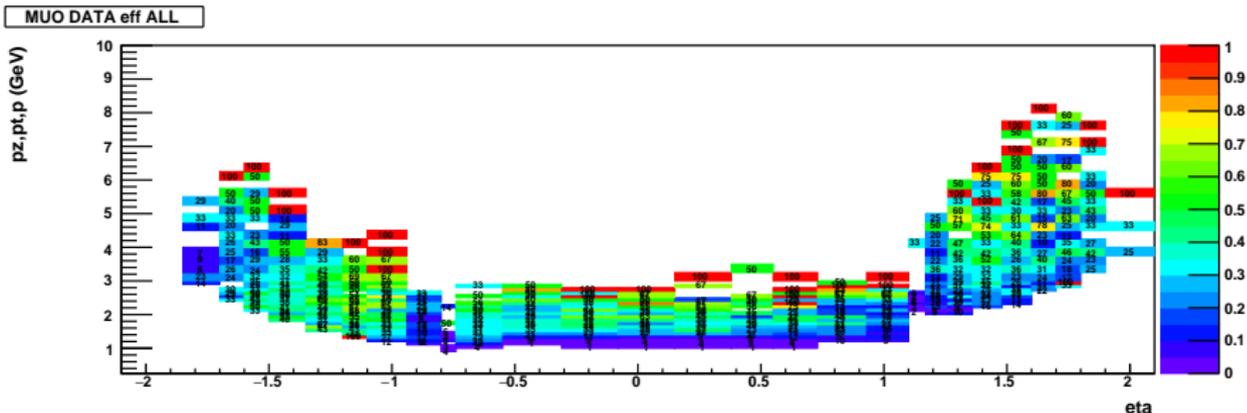
- **one step correction** for (FLT and SLT and TLT and off-line REC)
- separate maps for F/B/R/MUO, BAC and CAL (off-line only)
- evaluated for single muon **in $(p_{t_{eff}}, \eta)$ bins**, where as $p_{t_{eff}}$ is used:
(motivated by the CAL/BAC geometry and scaling of the muon path length)

- p in Forecap
- p_t in Barrel
- p_z in Rearcap

- proper identification of **the triggering muon** is crucial

- → the DATA/MC ratio delivers the correction weight: $\epsilon_x = \frac{\epsilon_{DATA}}{\epsilon_{MC}}$

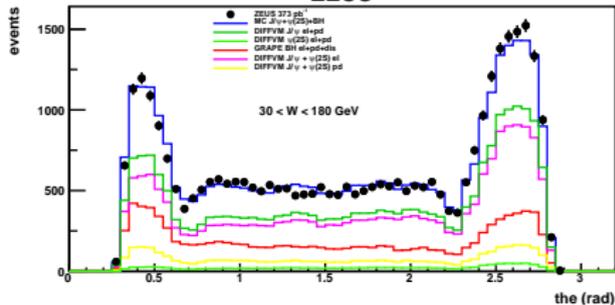
Muon correction maps: (p_z, p_t, p vs. η) - DATA



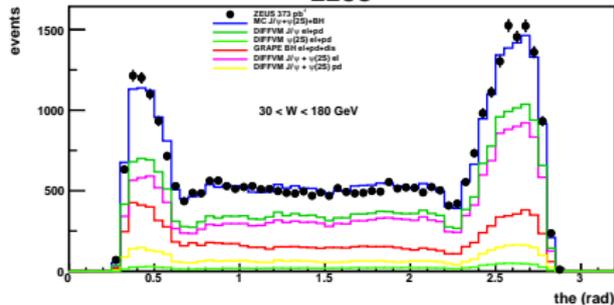
- muon tomography (+ muon range)
- probability (%) to fire FLT-SLT-TLT-REC chain by single muon on ($p_z, p_t, p; \eta$) grid
- X-axis (along eta): Rear-MUO, Barrel-MUO, Forward-MUO detectors
- only events with $M(\mu^+, \mu^-) < 6$ GeV
(ie. in the phase space range of di-muon mass fits)
- p_z, p_t, p grid: 100 MeV per bin ($p_{eff} < 3$ GeV), 250 MeV per bin ($p_{eff} > 3$ GeV)
- size of the grid is subject to systematics

θ and η distribution for μ^+ and μ^-

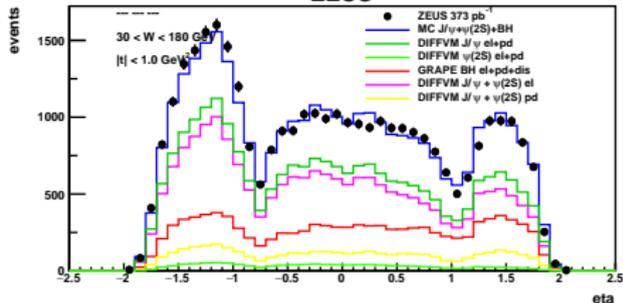
ZEUS



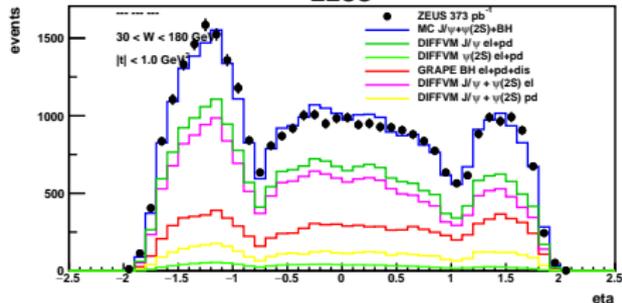
ZEUS



ZEUS

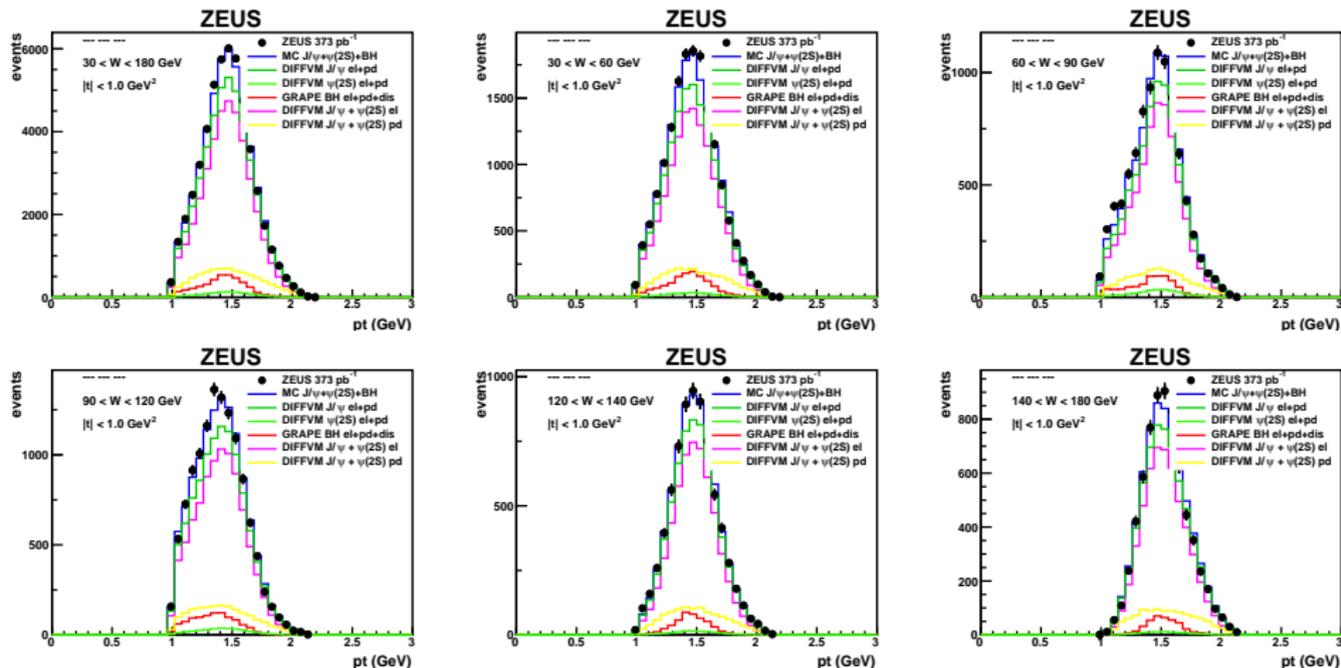


ZEUS



- θ and η distribution for muon tracks (μ^+ and μ^- , $\eta \in (-2, 2)$)
- after MC tuning and muon corrections
- well reproduced acceptance and efficiency of the detector

2-prongs: JPSI mass window: $p_t^{\mu^\pm}$ in W bins

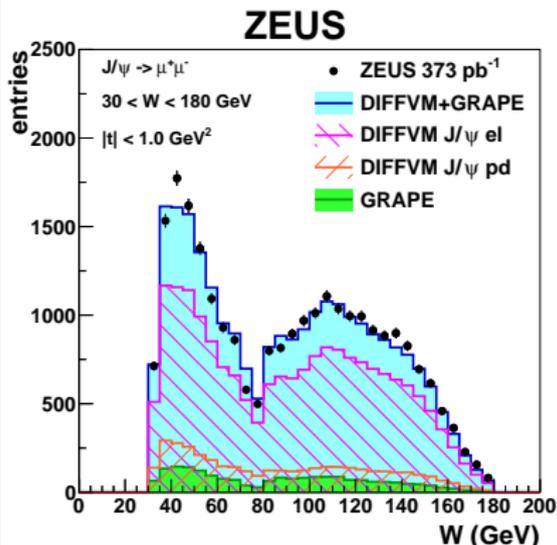


- ALL events and in W_1, W_2, W_3, W_4, W_5 bins
- **Jacobian peak around 1.5 GeV ($M_{JPSI}/2$)**
- almost no JPSI (and PSI2S) event loss due to the $p_t^{\mu^\pm} > 1$ GeV cut

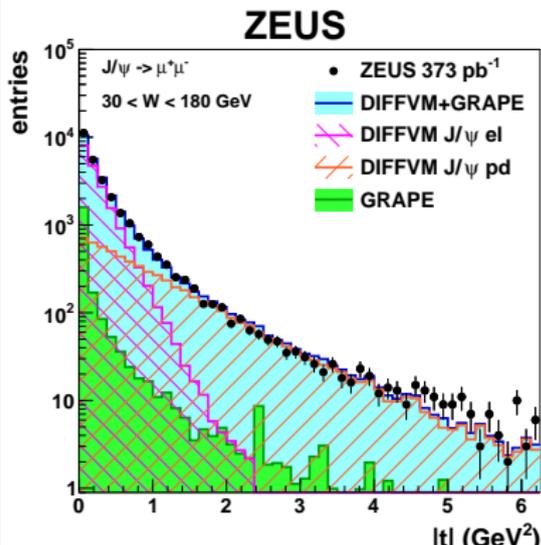
- W and $|t|$ distributions: 2-prongs

2-prongs: W and $|t|$ distributions: J/ψ mass window

W : $2.8 < M(\mu^+\mu^-) < 3.4$ GeV



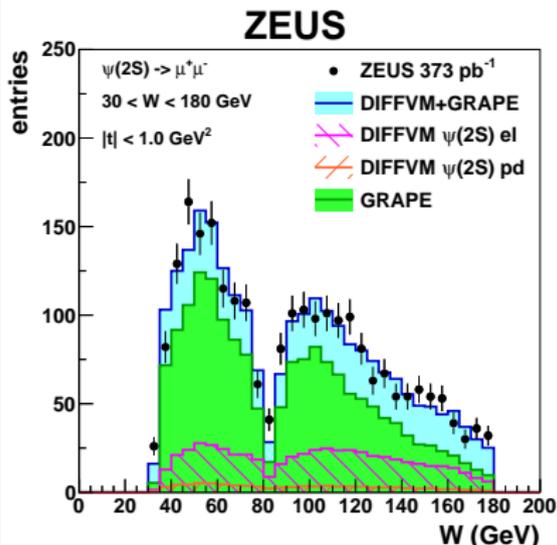
$|t|$: $2.8 < M(\mu^+\mu^-) < 3.4$ GeV



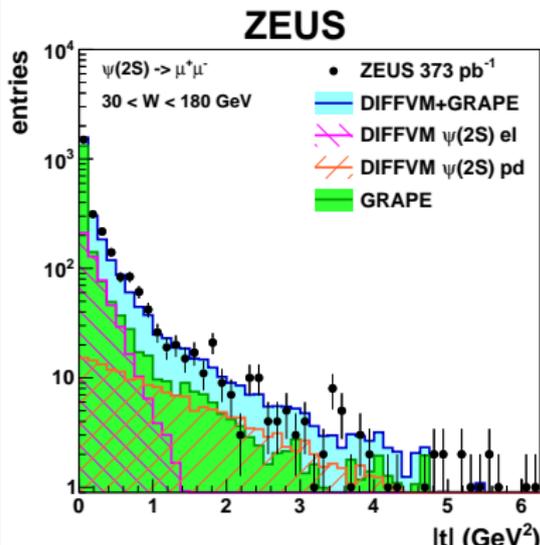
- dip in W distribution due to the anti-COSMIC cut: $\cos(\mu^+, \mu^-) < -0.985$
- proton dissociation dominates for $|t| > 1.0$ GeV²
- proton dissociative fraction: $f_{p,diss} = 0.17 \pm 0.01$ ($|t| < 1.0$ GeV²) from t -spectra fit

2-prongs: W and $|t|$ distributions: $\psi(2S)$ mass window

W : $3.4 < M(\mu^+\mu^-) < 4.0$ GeV



$|t|$: $3.4 < M(\mu^+\mu^-) < 4.0$ GeV



- dip in W distribution due to the anti-COSMIC cut: $\cos(\mu^+, \mu^-) < -0.985$
- proton dissociation dominates for $|t| > 1.0$ GeV²
- channel dominated by Bethe-Heitler continuum $\mu^+\mu^-$ background

- **Signal Extraction, Mass spectra**

2-prongs: Signal extraction: fit parameterization

- **Double Gaussian** shape: $G(x)$ or $g(x) = N \cdot \Delta \cdot \frac{1}{\sqrt{2\pi}\sigma} \exp\left(-\frac{(x-m)^2}{2\sigma^2}\right)$
where: N – number of events, Δ – mass bin width,
 m – mean value, σ – RMS

- for J/ψ : $N_1 \cdot G_1(x) + N_2 \cdot G_2(x)$

- for ψ' : $N'_1 \cdot g_1(x) + N'_2 \cdot g_2(x)$

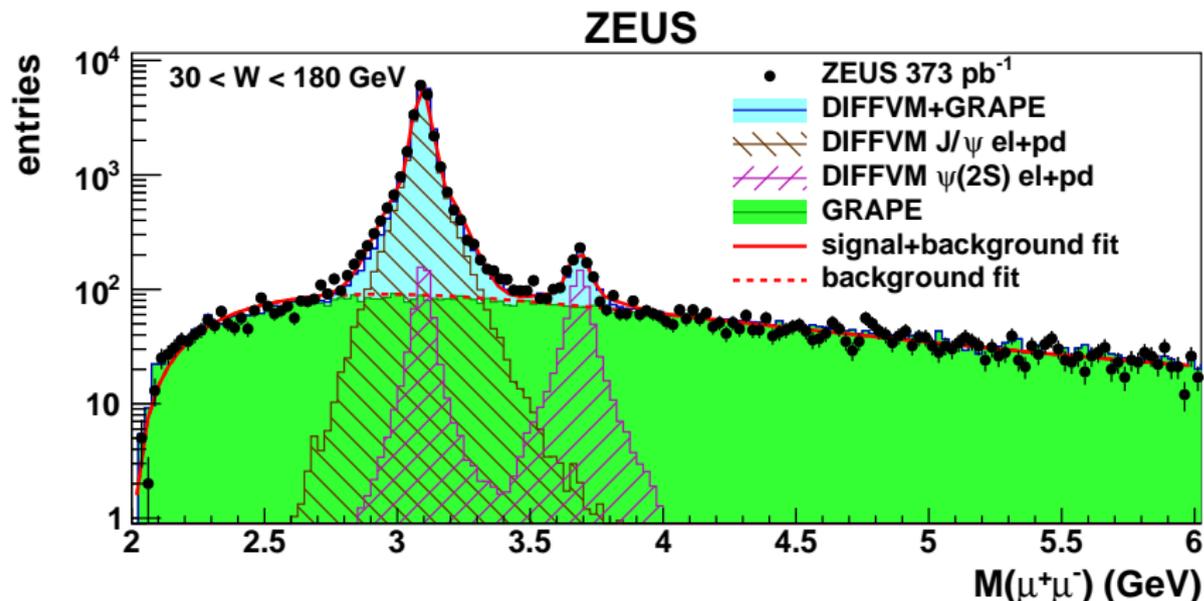
- introducing: $N = N_1 + N_2$, $N' = N'_1 + N'_2$, $R = \frac{N'}{N}$

- **with additional constraints**: $m_1 = m_2$, $m'_1 = m'_2$,
 $\frac{\sigma'_1}{\sigma_1} = \frac{\sigma'_2}{\sigma_2} = \alpha$, $\xi = \frac{N_1}{N} = \frac{N'_1}{N'}$ (**scaling of the mass resolution**)

- final formulae:

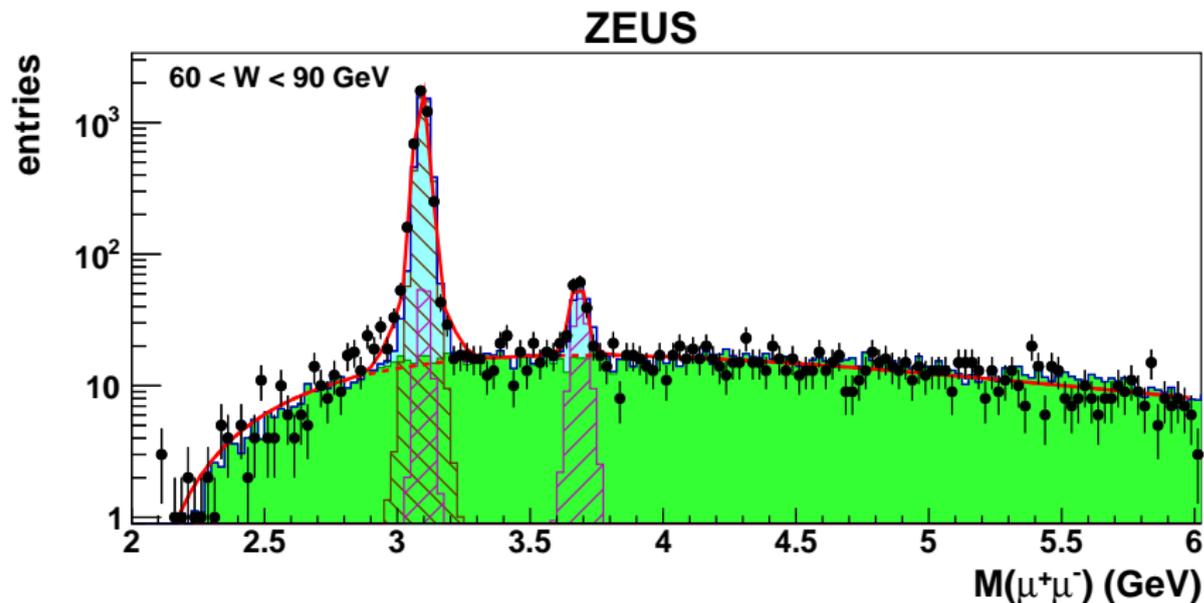
$$F(x) = N \cdot ((\xi \cdot G_1(x) + (1 - \xi) \cdot G_2(x)) + R \cdot (\xi \cdot g_1(x) + (1 - \xi) \cdot g_2(x))) + BG(x)$$

- **background function**: $BG(x) = A \cdot (x - B)^C \cdot \exp(-D(x - B) - E(x - B)^2)$
where A, B, C, D, E are fit parameters, B fixed ($= 2p_{t,min}^\mu$)

$M(\mu^+\mu^-)$ 

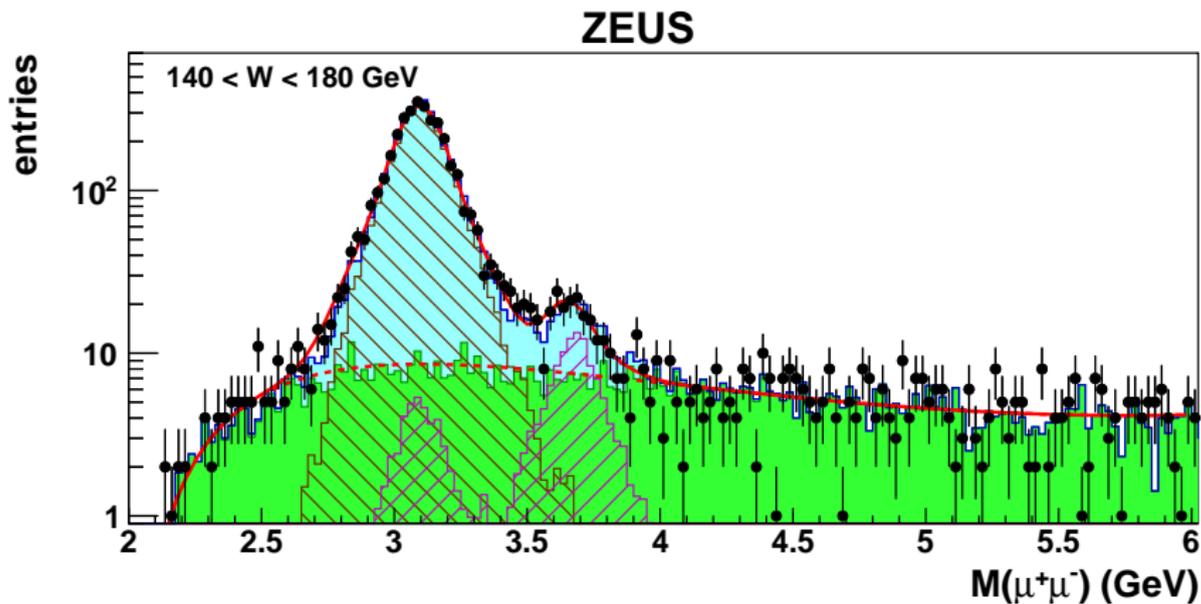
- full phase space: $30 < W < 180 \text{ GeV}$, $|t| < 1.0 \text{ GeV}^2$
- events yield: $\sim 23\,000 J/\psi$ and $\sim 700 \psi(2S)$
- resonant background under J/ψ peak

$M(\mu^+\mu^-)$



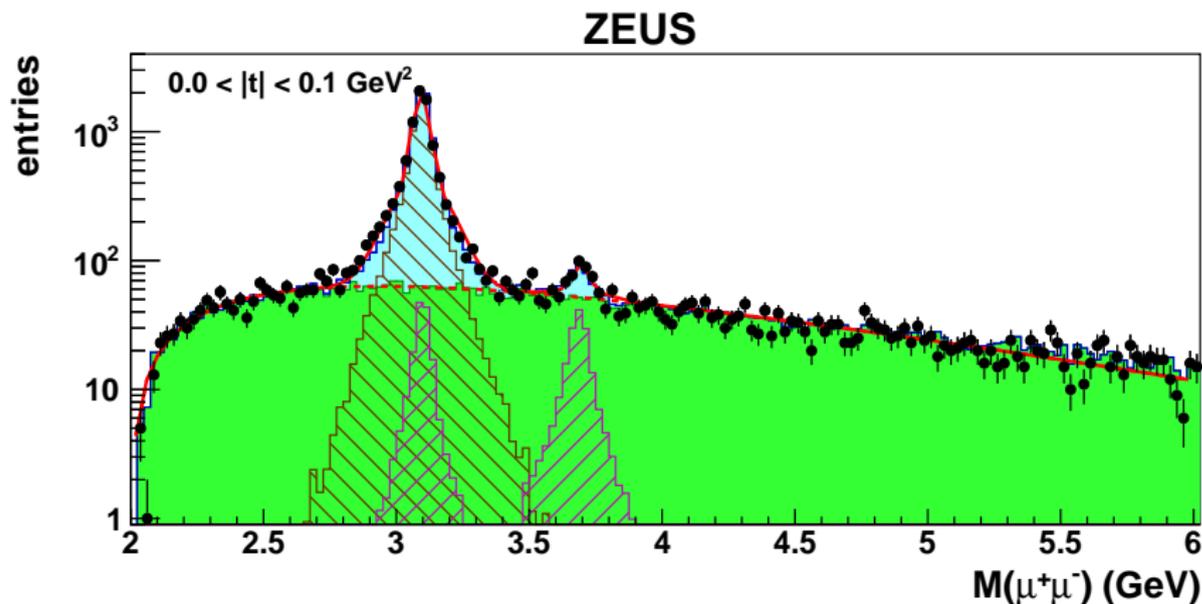
- **W2 bin:** $60 < W < 90$ GeV, $|t| < 1.0$ GeV²
- central rapidity region, long tracks, mass resolution: $\sigma_M(\mu\mu) \sim 22$ MeV

$$M(\mu^+\mu^-)$$



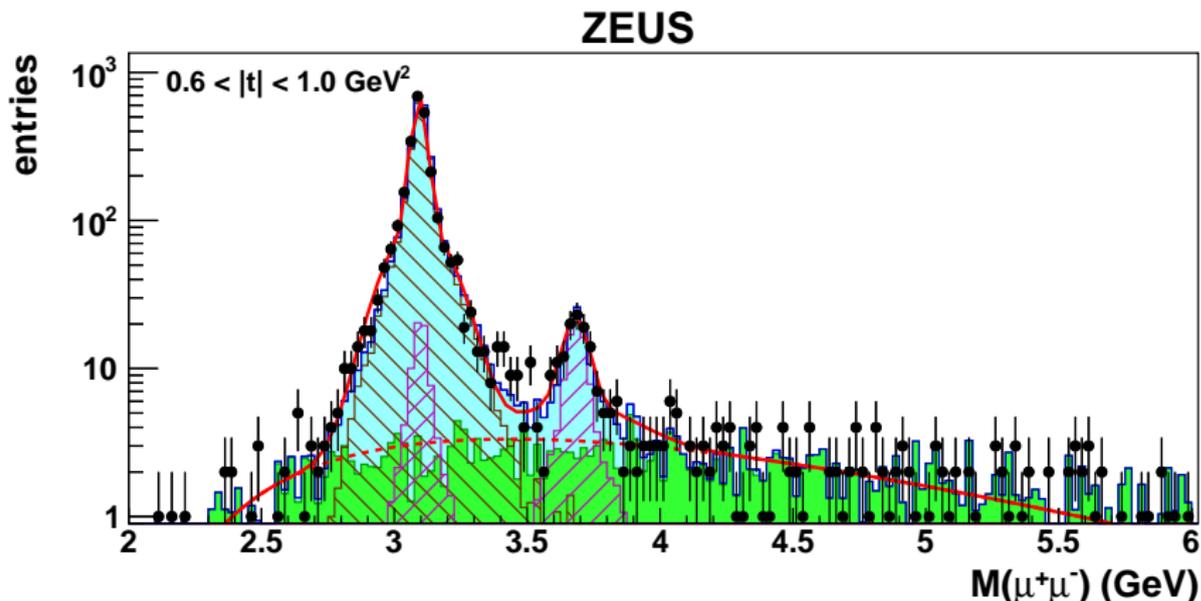
- **W5 bin:** 140 < W < 180 GeV, $|t| < 1.0 \text{ GeV}^2$
- high W, backward short tracks, mass resolution: $\sigma_M(\mu\mu) \sim 73 \text{ MeV}$

$M(\mu^+\mu^-)$



- **t1 bin:** $30 < W < 180 \text{ GeV}$, $|t| < 0.1 \text{ GeV}^2$
- low $|t|$, dominated by Bethe-Heitler continuum $\mu^+\mu^-$ background

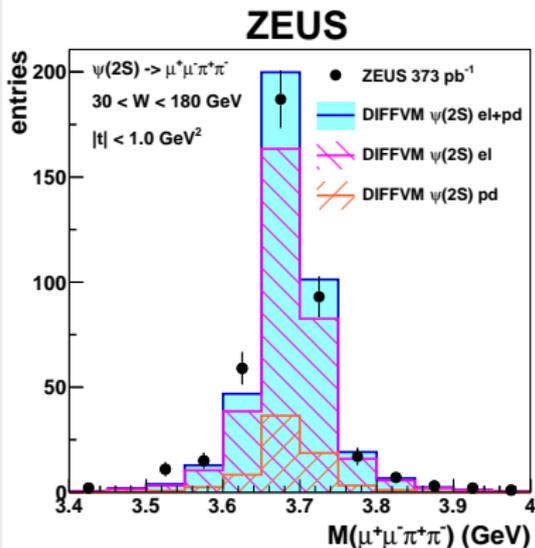
$M(\mu^+\mu^-)$



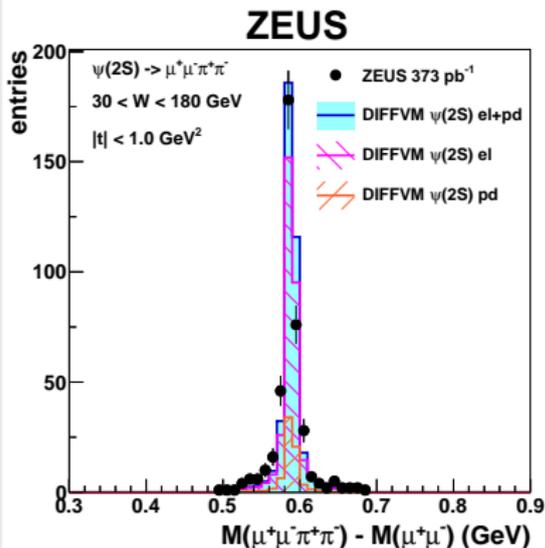
- **t5 bin:** $30 < W < 180 \text{ GeV}$, $0.6 < |t| < 1.0 \text{ GeV}^2$
- higher $|t|$, small Bethe-Heitler continuum $\mu^+\mu^-$ contribution
- **BUT:** high contamination proton dissociative events $\rightarrow \pi t$ -spectra

4-prongs: mass spectra: $\psi(2S) \rightarrow \mu^+\mu^-\pi^+\pi^-$

$$M(\mu^+\mu^-\pi^+\pi^-)$$



$$M(\mu^+\mu^-\pi^+\pi^-) - M(\mu^+\mu^-)$$

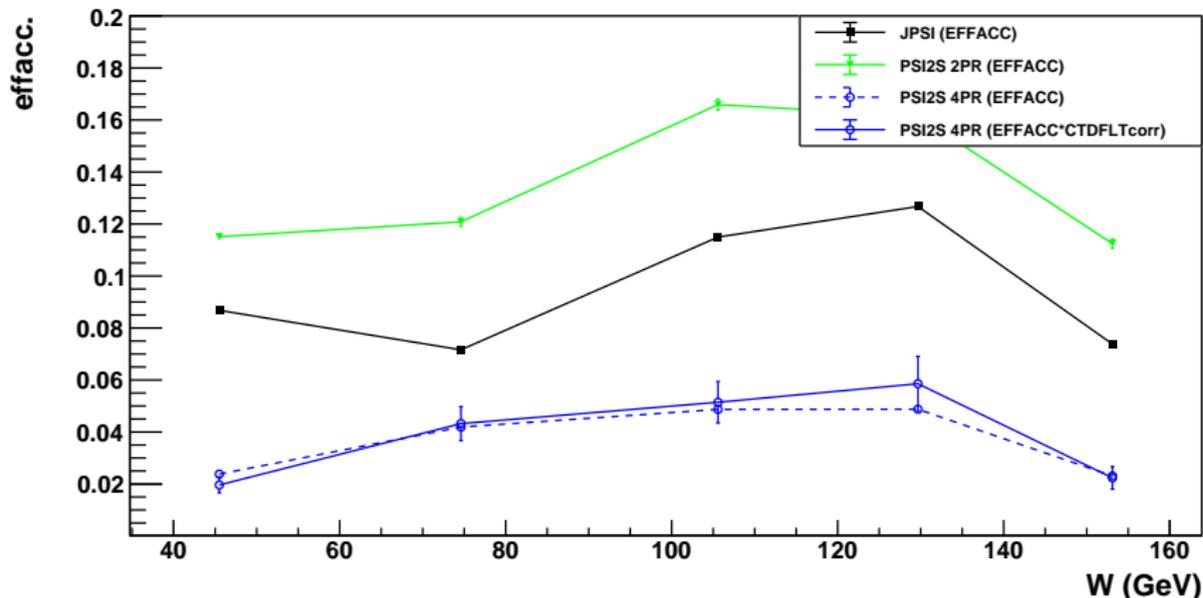


- events yield: $\sim 400 \psi(2S)$
- better resolution on mass difference \rightarrow cascade decay of $\psi(2S)$
- proton dissociative fraction: $f_{p,diss} = 0.16 \pm 0.01$ from t -spectra fit
- **almost background free channel**

- **selection efficiency**

Acceptance*efficiency in W bins: elastic

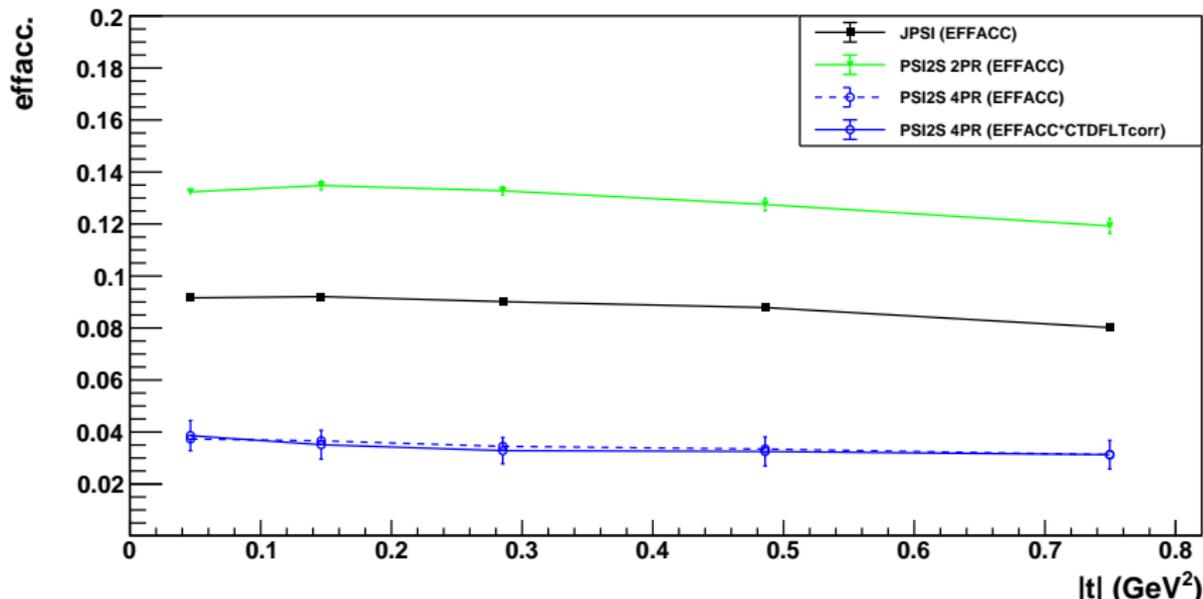
EFFACC (el) of JPSI, PSI2S-2PR, PSI2S-4PR vs. W



- JPSI, PSI2S 2- and 4-prong (2 ÷ 16%)
- Higher di-muon acceptance for higher mass state (PSI2S)
- similar angular coverage for final state di-muons
- second W bin (W_2) is the “dip” for di-muon acceptance

Acceptance*efficiency in $|t|$ bins: elastic

EFFACC (el) of JPSI, PSI2S-2PR, PSI2S-4PR vs. $|t|$



- JPSI, PSI2S 2- and 4-prong (4 ÷ 14%)
- Higher di-muon acceptance for higher mass state (PSI2S)
- flat in $|t|$ (no angular correlations to $|t|$)
- dashed line after CTD FLT corrections

- **Cross section ratio**

Cross section ratio $R = \frac{\sigma(\psi(2S))}{\sigma(J/\psi(1S))}$, full kinematic range

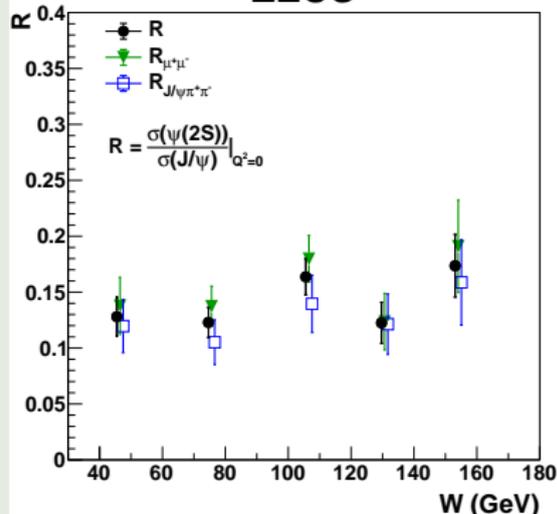
$30 < W < 180$ GeV, $|t| < 1.0$ GeV², $Q^2 < 1.0$ GeV²

$\psi(2S)$ decay mode	$R = \frac{\sigma(\psi(2S))}{\sigma(J/\psi(1S))}$
$\mu^+ \mu^-$	0.154 ± 0.012
$J/\psi(\rightarrow \mu^+ \mu^-) \pi^+ \pi^-$	0.125 ± 0.019
combined	$0.146 \pm 0.010^{+0.016}_{-0.020}$

- $$R_{J/\psi\pi\pi} = \frac{N_{\psi(2S)}}{N_{J/\psi(1S)}} \cdot \frac{Acc_{J/\psi(1S) \rightarrow \mu^+ \mu^-}}{Acc_{\psi(2S) \rightarrow J/\psi\pi^+\pi^-}} \cdot \frac{1}{BR_{\psi(2S) \rightarrow J/\psi\pi^+\pi^-}} \cdot \frac{1 - f_{p.diss}^{\psi(2S)}}{1 - f_{p.diss}^{J/\psi(1S)}}$$
- $$R_{\mu\mu} = \frac{N_{\psi(2S)}}{N_{J/\psi(1S)}} \cdot \frac{Acc_{J/\psi(1S) \rightarrow \mu^+ \mu^-}}{Acc_{\psi(2S) \rightarrow \mu^+ \mu^-}} \cdot \frac{BR_{J/\psi(1S) \rightarrow \mu^+ \mu^-}}{BR_{\psi(2S) \rightarrow \mu^+ \mu^-}} \cdot \frac{1 - f_{p.diss}^{\psi(2S)}}{1 - f_{p.diss}^{J/\psi(1S)}}$$
- $Acc_i = \frac{N_i^{reco}}{N_i^{true}}, f_{p.diss}^i$ - fraction of proton dissociative events
- $BR(\psi(2S) \rightarrow J/\psi\pi^+\pi^-) = (34.68 \pm 0.3)\%$, $BR(\psi(2S) \rightarrow \mu^+\mu^-) = (0.80 \pm 0.06)\%$,
 $BR(J/\psi \rightarrow \mu^+\mu^-) = (5.961 \pm 0.033)\%$, $BR(\psi(2S) \rightarrow \mu^+\mu^-\pi^+\pi^-) = (2.07 \pm 0.02)\%$ (PDG 2020)
- both channels have similar precision and provide consistent results**

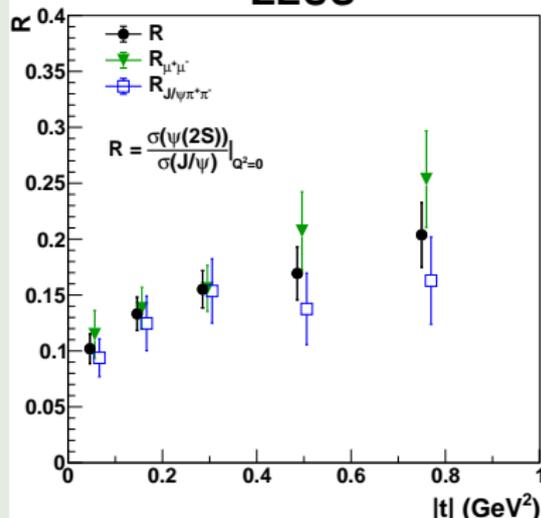
R vs. W

ZEUS



R vs. $|t|$

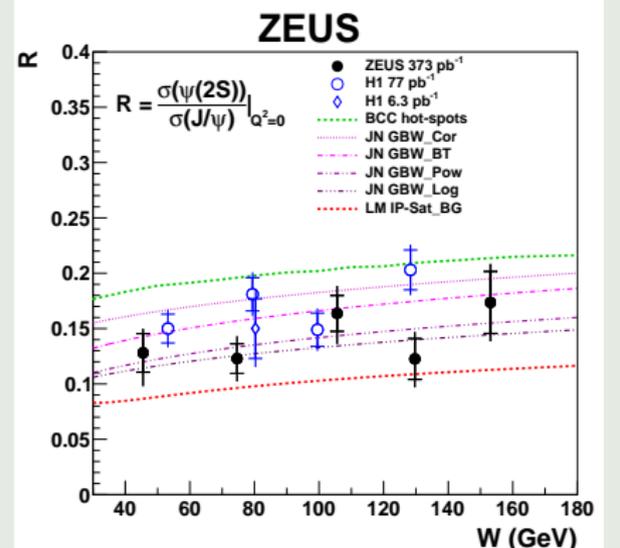
ZEUS



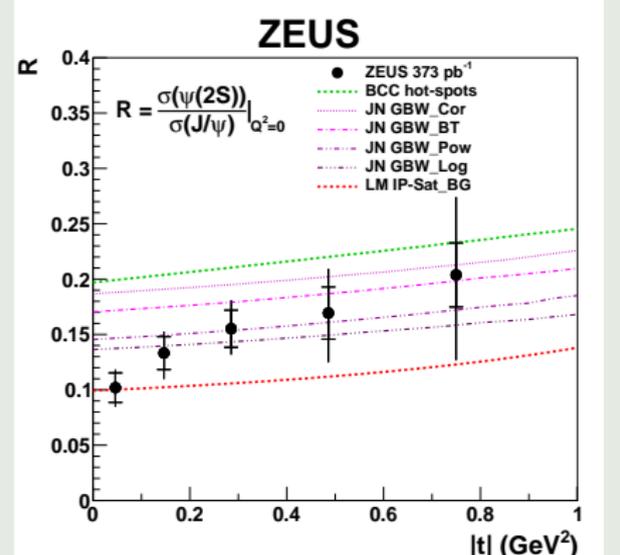
- $R_{\mu\mu}$ (2-prongs channel), $R_{J/\psi\pi\pi}$ (4-prongs channel) and combined R (full dots)
- statistical errors only
- **good agreement between two channels**

cross section ratio $R = \sigma_{\psi(2S)}/\sigma_{J/\psi(1S)}$: Final Results

R vs. W



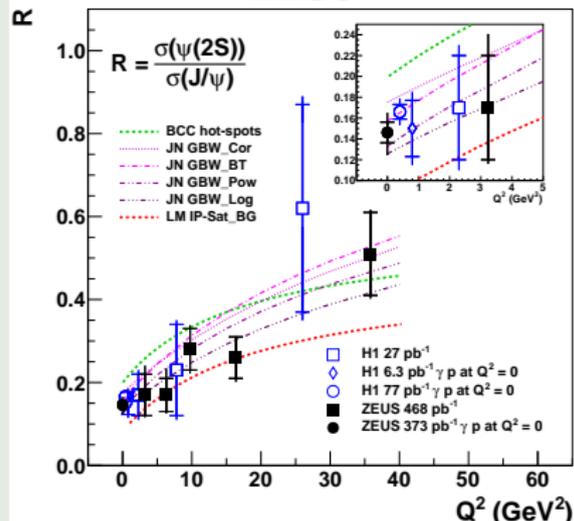
R vs. $|t|$



- for R vs. W ZEUS (full dots) and H1 (open markers) results are compared
- **no W dependence observed, moderate increase with $|t|$**
- good agreement between data and theoretical models (see next page)
- errors at high- $|t|$ points dominated by systematics (\rightarrow proton dissociative fraction)

R vs. Q^2

ZEUS



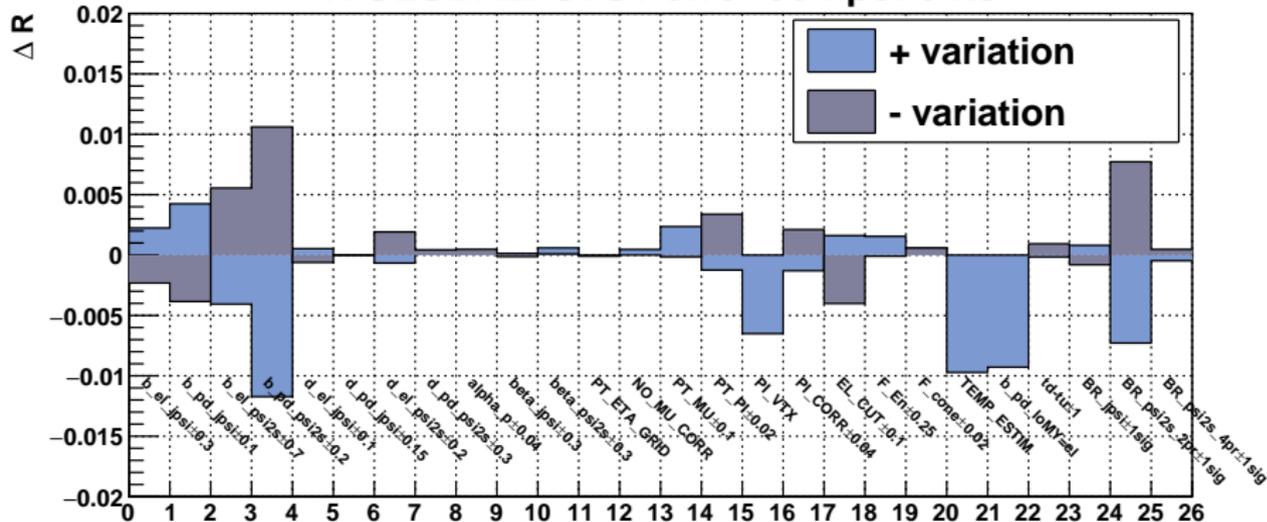
theoretical models:

- Bendova, Cepila and Contreras (BCC hot-spots):
 - Phys. Rev. D **99**, 034025 (2019).
- Jan Nemchik et al. (JN):
 - Eur. Phys. J. C **79**, 154 (2019).
 - Eur. Phys. J. C **79**, 495 (2019).
 - Phys. Rev. D **103**, 094027 (2021).
- Lappi and Mäntysaari (LM IP-Sat):
 - Phys. Rev. C **83**, 065202 (2011).
 - Phys. Rev. D **87**, 034002 (2013).
 - PoS (DIS2014), 069 (2014).

- ZEUS (full dot) and H1 (open markers) photoproduction results plotted at $Q^2 \sim 0$
- DIS results are also presented vs. Q^2 : ZEUS (full squares) and H1 (open squares)
- good agreement between data and theoretical models (\rightarrow backup plots, page 52)
- **better precision of photoproduction points**

h_SYST_TOT_0

R GLOBAL: SYST error components



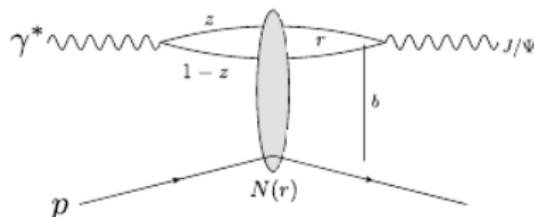
- biggest contributions from:
- b -slope variation of t -dependence (esp. for b_{pd} of $\psi(2S)$) → p.diss fraction
- event number estimator (MC templates fit instead of Gaussian fit) → BH bckgr.
- slow pions vertexing → very soft tracks reconstruction
- $BR(\psi(2S) \rightarrow \mu^+ \mu^-)$ → PDG world average...

- **Theoretical Models: Color Dipole**

Fluctuations and diffractive vector meson production

High energy factorization:

- ① $\gamma^* \rightarrow q\bar{q}$ splitting,
wave function $\Psi^\gamma(r, Q^2, z)$
- ② $q\bar{q}$ dipole scatters elastically:
 $N(r, x, b)$
- ③ $q\bar{q} \rightarrow J/\Psi$,
wave function $\Psi^V(r, Q^2, z)$



Diffractive scattering amplitude

$$A \sim \int d^2b dz d^2r \Psi^{\gamma^*}(r, Q^2, z) e^{-ib \cdot \Delta} N(r, x, b)$$

- Impact parameter is the Fourier conjugate to the momentum transfer ($-t \approx \Delta^2$) \rightarrow **access to the spatial structure**

This is LO, see Jani's talk for NLO corrections!

Incoherent Scattering

Good, Walker (Phys. Rev. 120 (1960) 1857–1860):

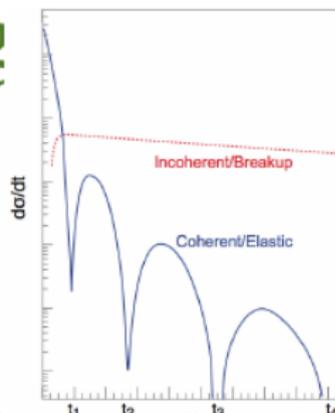
Proton dissociates ($f \neq i$):

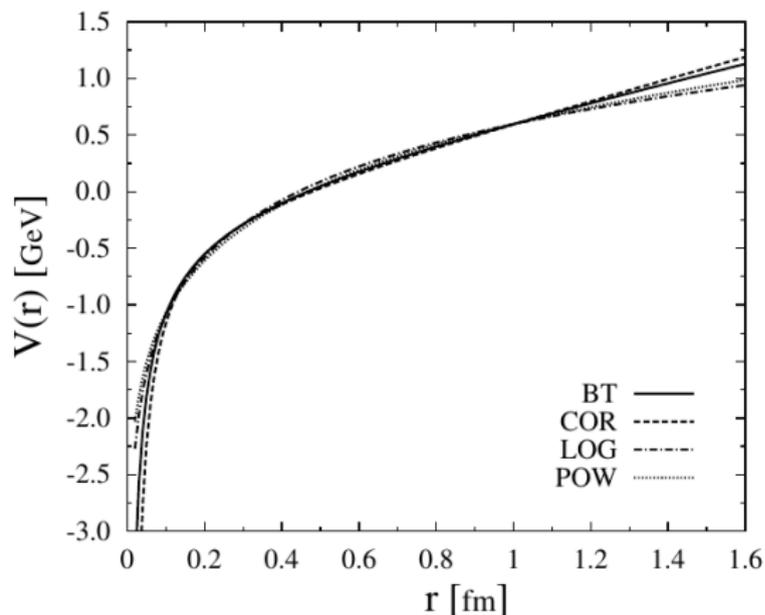
$$\begin{aligned} \sigma_{\text{incoherent}} &\propto \sum_{f \neq i} \langle i | \mathcal{A} | f \rangle^\dagger \langle f | \mathcal{A} | i \rangle \quad \text{complete set} \\ &= \sum_f \langle i | \mathcal{A} | f \rangle^\dagger \langle f | \mathcal{A} | i \rangle - \langle i | \mathcal{A} | i \rangle^\dagger \langle i | \mathcal{A} | i \rangle \\ &= \langle i | |\mathcal{A}|^2 | i \rangle - |\langle i | \mathcal{A} | i \rangle|^2 = \langle |\mathcal{A}|^2 \rangle - |\langle \mathcal{A} \rangle|^2 \end{aligned}$$

The incoherent CS is the variance of the amplitude!!

$$\frac{d\sigma_{\text{total}}}{dt} = \frac{1}{16\pi} \langle |\mathcal{A}|^2 \rangle$$

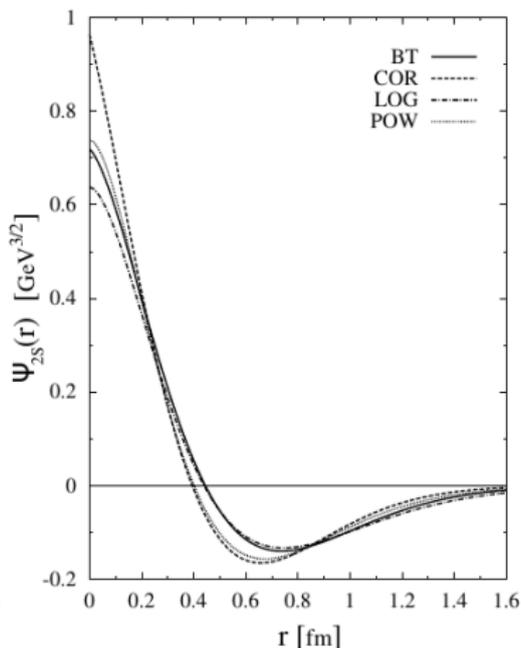
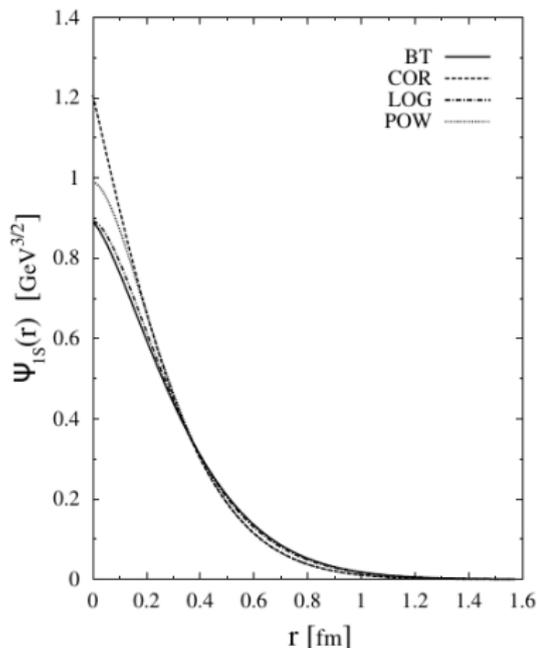
$$\frac{d\sigma_{\text{coherent}}}{dt} = \frac{1}{16\pi} |\langle \mathcal{A} \rangle|^2$$





- **COR**: Cornell potential and **BT**: Buchmüller and Tye : $V(r) = -\frac{k}{r} + \frac{r}{a^2}$,
 $k = 0.52$, $a = 2.34 \text{ GeV}^{-1}$, $m_c = 1.84 \text{ GeV}$ (**BT**: $m_c = 1.48 \text{ GeV}$)
- **LOG**: Logarithmic potential: $V(r) = 0.6635 \text{ GeV} + (0.733 \text{ GeV})\log(r \cdot 1 \text{ GeV})$
- **POW**: Power-law potential: $V(r) = 8.064 \text{ GeV} + (6.898 \text{ GeV})(r \cdot 1 \text{ GeV})^{0.1}$,
 $m_c = 1.8 \text{ GeV}$

radial wave functions for $J/\psi(1S)$ and $\psi(2S)$



- radial part of the wave functions $\Psi(r)$ for $c\bar{c}$ 1S and 2S states

- $(\frac{\Delta}{m_c} + V(r))\Psi_{nlm}(\vec{r}) = E_{nl}\Psi_{nlm}(\vec{r})$, $\Psi_{nlm}(\vec{r}) = \Psi_{nl}(r) \cdot Y_{lm}(\theta, \phi)$

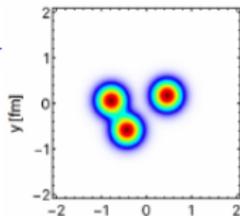
- BT, COR, LOG, POW potentials

- **Theoretical Models: Gluon Hot Spots**

Incoherent Scattering in ep

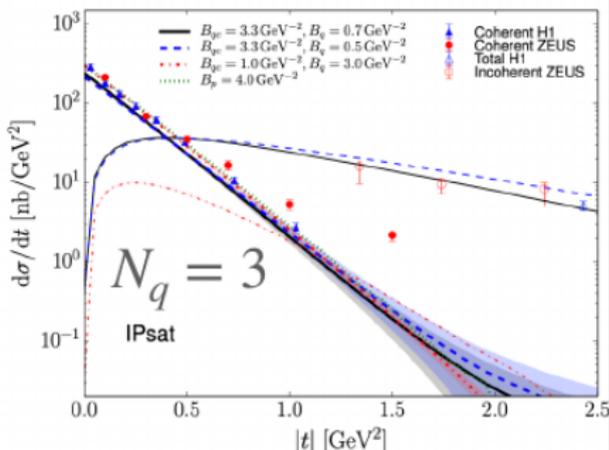
$$\frac{d\sigma_{q\bar{q}}}{d^2\mathbf{b}} = 2 \left[1 - \exp \left(-\frac{\pi^2}{2N_c} r^2 \alpha_s(\mu^2) xg(x, \mu^2) T(b) \right) \right]$$

$$T_p(b) = \frac{1}{2\pi B_G} e^{-\frac{b^2}{2B_G}}$$



$$T_p(b) = \frac{1}{2\pi N_q B_q} \sum_{i=1}^{N_q} e^{-\frac{(\vec{b} - \vec{b}_i)^2}{2B_q}}$$

\vec{b}_i with a Gaussian distribution of width B_{qc}



Also: large scale (small $|t|$) saturation scale fluctuations.

• Arjun Kumar, Tobias Toll : arXiv:2202.06631

- **Cross section ratio $R = \frac{\sigma(\psi(2S))}{\sigma(J/\psi(1S))}$** in photoproduction using HERA II data was measured by ZEUS in the kinematic range: $30 < W < 180$ GeV, $|t| < 1.0$ GeV²
- first ZEUS measurement of R in photoproduction (at $Q^2 = 0$):
 $R = 0.146 \pm 0.01(\text{stat.})_{-0.022}^{+0.016}(\text{syst.})$
- first HERA result for R vs. $|t|$ in photoproduction
- **moderate rise of cross section ratio as a function of $|t|$**
- **no W dependence observed within experimental errors**
- consistent results for 2- and 4-prongs decay channels
- comparable precision in both decay channels
- **theoretical calculations of the ratio $\frac{\sigma(\psi(2S))}{\sigma(J/\psi(1S))}$ for exclusive vector-meson production has been compared to the experimental data**
- **→ majority of the predictions are consistent with the data**
- **data start to exhibit constraining power**

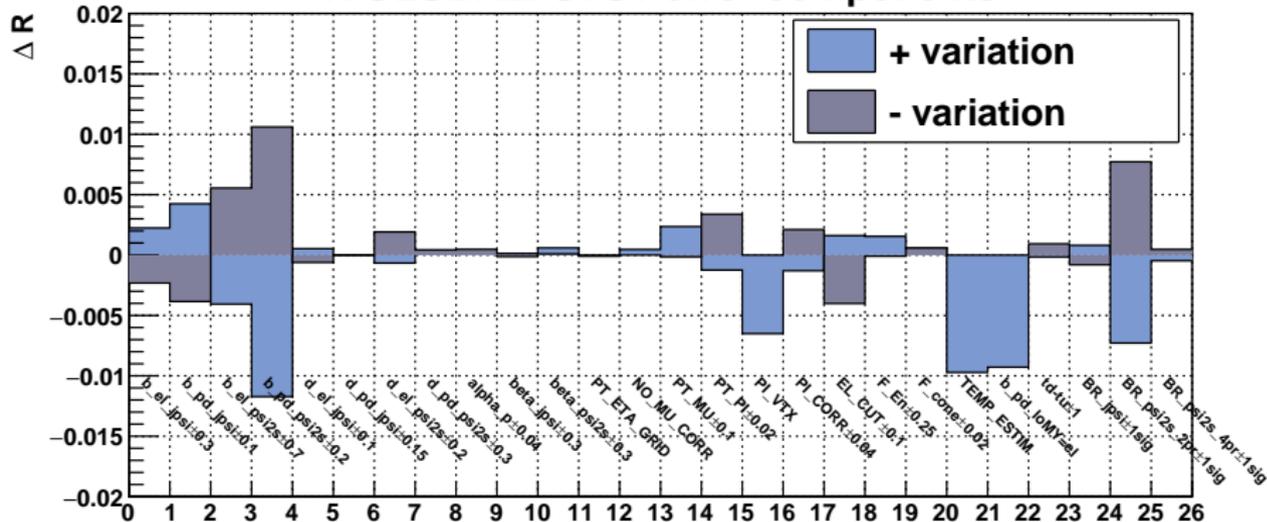
Thank You For Your Attention

BACKUP PLOTS FOLLOWS...

- **Systematics**

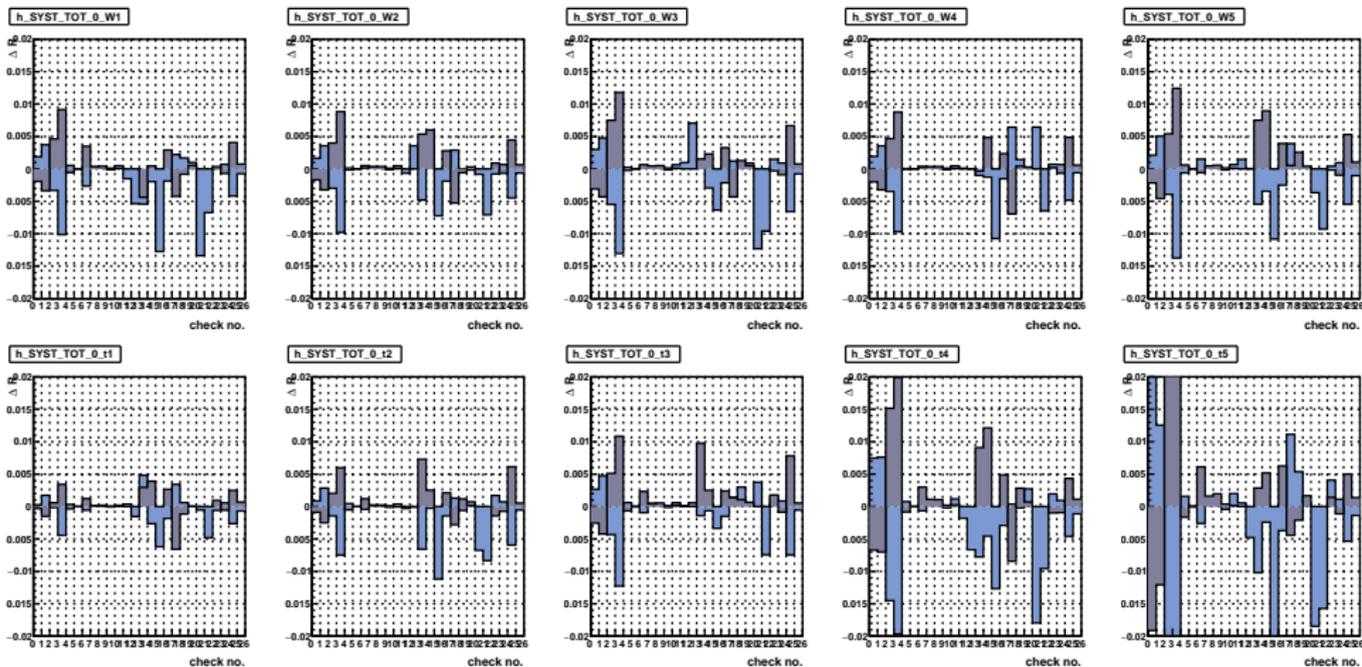
h_SYST_TOT_0

R GLOBAL: SYST error components



- biggest contributions from:
- b -slope variation of t -dependence (esp. for b_{pd} of $\psi(2S)$) → **p.diss fraction**
- event number estimator (MC templates fit instead of Gaussian fit) → **BH bckgr.**
- slow pions vertexing → **very soft tracks reconstruction**
- $BR(\psi(2S) \rightarrow \mu^+ \mu^-)$ → **PDG world average...**

R: components of SYST. error in W and $|t|$ bins



- upper row: contributions in 5 W bins
- bottom row: contributions in 5 $|t|$ bins
- bin order as on previous page

- **Selection cuts**

- **Exclusive Muon Triggers** (F/B/R/MUON or BAC)
- **Tracking and Vertex**
 - $N_{track} = 2$, oppositely charged tracks matched to the primary vertex ($\eta \in (-1.9, 1.9)$)
 - **both tracks identified as a muon in CAL, at least one in F/B/RMUON or BAC**
 - $p_T > 1.0$ GeV of each track
 - anti-COSMIC cuts (CAL timing, acolinearity: $\cos(\mu^+, \mu^-) < -0.985$)
- **Elasticity/Exclusivity and Photoproduction cuts** (on CAL Energy)
 - no scattered electron found in CAL
 - $E_{clu} < 0.5$ GeV for clusters not matched to muons (or pions)
(corresponds to an effective cut on $Q^2 < 1$ GeV²)
 - $E(\theta < 0.12rad) < 1$ GeV
the sum of the energy in the FCAL cone around the beam-pipe;
to suppress proton-dissociative events, $ep \rightarrow e + VM + Y$
(corresponds to a requirement for $M_Y \lesssim 5$ GeV)
- **Kinematic range (analysis phase space):**
 - $30 < W < 180$ GeV
 - $|t| < 1.0$ GeV²
 - $Q^2 < 1$ GeV² (median $Q^2 \approx 3 \times 10^{-5}$ GeV²)

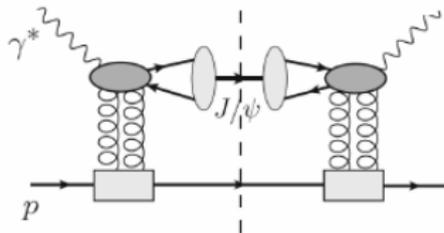
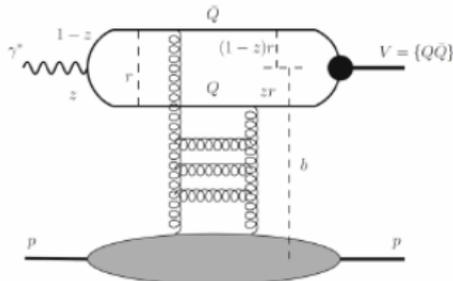
- (only differences w.r.t. the 2-prong channel)
- $N_{track} = 4$, (two oppositely charged pairs, sorted by p_T)
- **highest momentum pair: muon candidates**
lowest momentum pair: pion candidates
- no anti-COSMIC cuts
- transverse momentum of pion candidates: $p_T^\pi > 0.12$ GeV;
- $2.8 < M(\mu^+ \mu^-) < 3.4$ GeV (J/ψ window)
- $M(\mu^+ \mu^- \pi^+ \pi^-) - M(\mu^+ \mu^-)$ in (0.5 – 0.7) GeV window
(**cascade decay of $\psi(2S)$**)

- **Theoretical Models**

- predictions of all models were calculated within the phase space of this analysis:
 - $30 < W < 180$ GeV
 - $|t| < 1.0$ GeV²
 - $Q^2 \sim 0$ (photoproduction points)

- **Jan Nemchik (JN) et al. :**
- Eur. Phys. J. C **79**, no.6, 495 (2019).
- Eur. Phys. J. C **79**, no.2, 154 (2019).
- calculations have been performed for various combinations of quarkonium wave functions:
 - **Cor** (Cornell potential)
 - **BT** (Buchmüller-Tye)
 - **Pow** (Power-law potential)
 - **Log** (Logarithmic potential)
- and models for the dipole cross sections:
 - BGBK, **GBW** ← **used on the plots**
 - for each combinations calculations are performed with and w/o skewness in the gluon density
- the same b -slope parameters for both quarkonium states

Color dipole formalism for VM



Amplitude:

$$\mathcal{A}^{\gamma^* p \rightarrow Vp}(x, Q^2, \vec{q}) = \langle V | \tilde{\mathcal{A}} | \gamma^* \rangle = \int d^2r \int_0^1 d\alpha \Psi_V^*(\vec{r}, \alpha) \mathcal{A}_{Q\bar{Q}}(\vec{r}, x, \alpha, \vec{q}) \Psi_{\gamma^*}(\vec{r}, \alpha, Q^2)$$

t-dependent differential cross section:

$$\frac{d\sigma^{\gamma^* p \rightarrow Vp}(s, Q^2, t = -q^2)}{dt} = \frac{1}{16\pi} \left| \mathcal{A}^{\gamma^* p \rightarrow Vp}(s, Q^2, \vec{q}) \right|^2$$

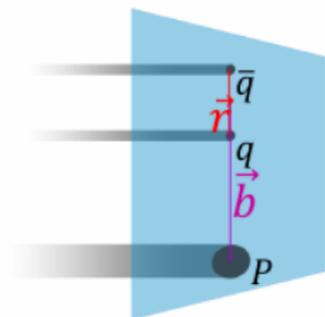


Dipole cross section

- Describes the **interaction** of $q\bar{q}$ with a **proton**
- **Nonperturbative effects, no theoretically calculable**
- **Just models**
 - Nevertheless, qualitatively, we have ideas, what is going inside
 - In the perturbative area described by the **gluon distribution function**
- Various models on the market: **GBW, KST, IP-Sat, BGBK, BK, ...**
- Usually, they are **fitted from DIS data, mostly from HERA**
- However, such a fit **is integrated over impact parameter \vec{b}**
- For t -dependence, **we need a b -dependent dipole cross section (amplitude)**

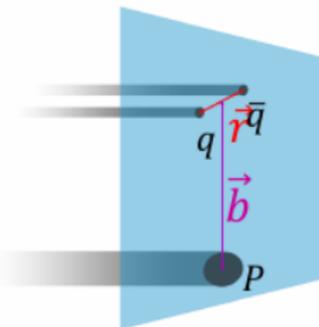
More in B.Kopeliovich, MK, J.Nemchik, Phys.Rev.D 103 (2021) 9, 094027

$\vec{b}-\vec{r}$ correlation



This is the case of **maximal contribution**.

$\vec{b} \parallel \vec{r}$ is simpler to calculate, no angle dependence.



Solution: Inspired by the Born approximation with two-gluon exchange

In reality, the angle between $\vec{b}-\vec{r}$ can be arbitrary.

One should integrate over all possibilities.

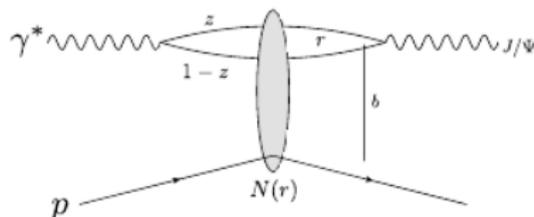
This is a challenge e.g. for BK. So far, only the $\vec{b} \parallel \vec{r}$ approximation was used.

More in B.Kopeliovich, MK, J.Nemchik, Phys.Rev.D 103 (2021) 9, 094027 & DIS2021

Fluctuations and diffractive vector meson production

High energy factorization:

- ① $\gamma^* \rightarrow q\bar{q}$ splitting,
wave function $\Psi^\gamma(r, Q^2, z)$
- ② $q\bar{q}$ dipole scatters elastically:
 $N(r, x, b)$
- ③ $q\bar{q} \rightarrow J/\Psi$,
wave function $\Psi^V(r, Q^2, z)$



Diffractive scattering amplitude

$$A \sim \int d^2b dz d^2r \Psi^{\gamma^*} \Psi^V(r, Q^2, z) e^{-ib \cdot \Delta} N(r, x, b)$$

- Impact parameter is the Fourier conjugate to the momentum transfer ($-t \approx \Delta^2$) \rightarrow **access to the spatial structure**

This is LO, see Jani's talk for NLO corrections!

Diffractive vector meson production

Coherent

$$\sigma_{\text{coherent}} \sim |\langle \mathcal{A} \rangle_{\Omega}|^2$$

- Proton stays intact

Probes the average interaction

⇒ average shape

- Experimental signature: rapidity gap
- Theoretically: no net color transfer
- Average over target configurations Ω at amplitude/cross section level

Incoherent

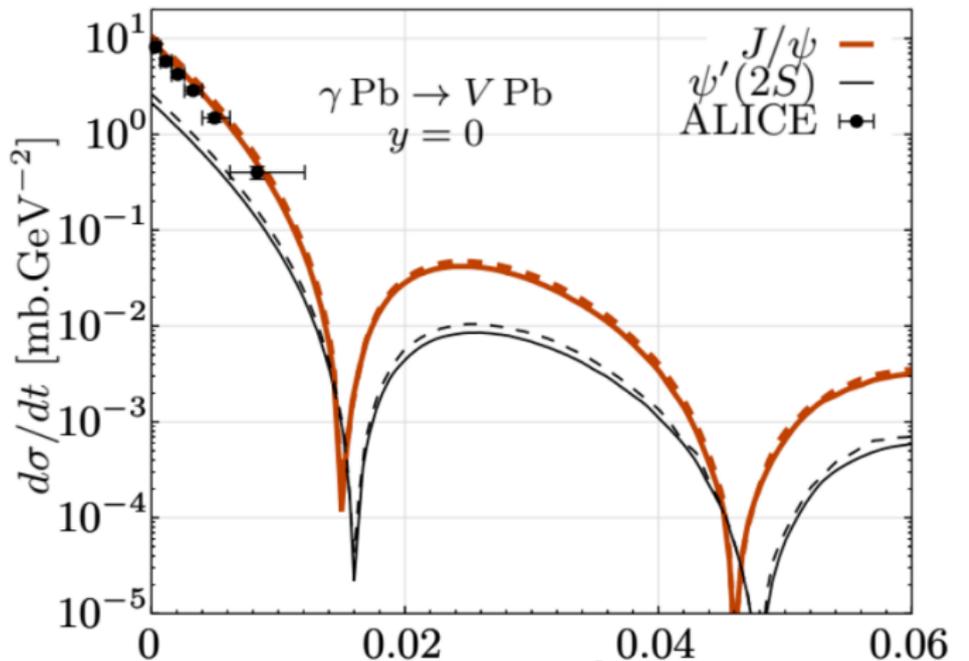
$$\sigma_{\text{incoherent}} \sim \langle |\mathcal{A}|^2 \rangle_{\Omega} - |\langle \mathcal{A} \rangle_{\Omega}|^2$$

- Proton dissociates

Event-by-event fluctuations in the proton structure

$$\mathcal{A}^{\gamma^* p \rightarrow V p} \sim \int d^2\mathbf{b} d^2\mathbf{z} d^2\mathbf{r} \Psi^{\gamma^*} \Psi^V(|\mathbf{r}|, z, Q^2) e^{-i\mathbf{b} \cdot \mathbf{\Delta}} N(|\mathbf{r}|, x, \mathbf{b}, \Omega)$$

Miettinen, Pumplin, PRD 18, 1978; Caldwell, Kowalski, 0909.1254; H.M., Schenke, 1603.04349; H.M., 2001.10705

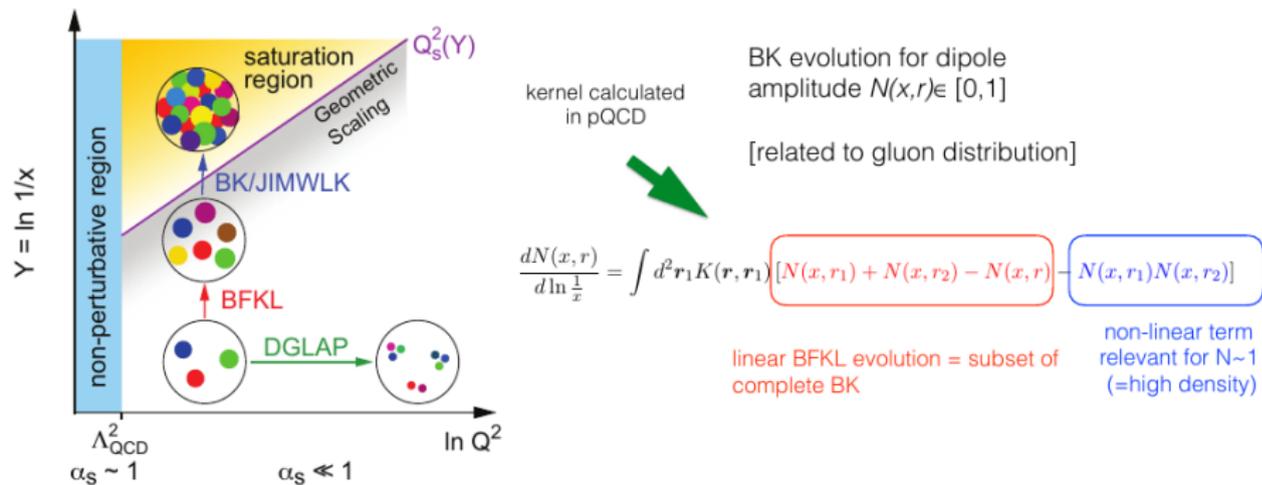


- \sim Fourier transform of the spatial gluon density distribution
- higher maxima hidden by proton-dissociative background
- excellent resolution for t reconstruction needed !

- **Lappi and Mntysaari (LM IP-Sat) :**
- the BFKL evolution plus the IP-Sat model to predict vector-meson production in ep and electronion collisions in the dipole picture
- 2S parameters from arXiv:1406.2877 (PoS DIS2014 (2014) 069)
- 1S parameters from hep-ph/0606272 (Phys.Rev. **D74** (2006) 074016)
- Calculation described in (Phys.Rev. **C83** (2011) 065202)
- **IP-Sat** dipole from fit (Phys.Rev. **D87** (2013) no.3, 034002)
- Wave function: Boosted Gaussian (**BG**), $Q^2 = 0 \text{ GeV}^2$
- Skewedness and real part corrections included

- **Bendova, Cepila and Contreras (BCC hot-spots) :**
- Phys. Rev. D **99**, 034025 (2019).
- model with hot spots randomly sampled in the transverse plane bound by the size of the proton
- The slope parameter b is 4.72 GeV^{-2} and it is fixed by the combined H1 and ZEUS data from 2013 for J Ψ photoproduction t -distribution.
- the same b -slope for both J Ψ and $\Psi(2S)$

Goal: confront linear vs. non-linear QCD evolution



- Nuclear Amplitude $N(x,r)$

Modelling x-dependence:

1. The Proton's Size

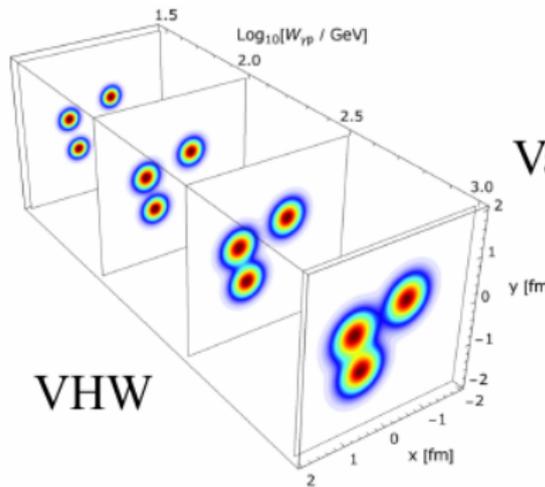
$$T_p(b) = \frac{1}{2\pi B_G} e^{-\frac{b^2}{2B_G}}$$

$$B_G(x_{IP}) = B_p x_{IP}^{\lambda_p}$$

$$r_{\text{rms}} = \sqrt{2B_G(x_{IP})}$$

Modelling x-dependence:

2. The Hotspot Size



$$T_p(b) = \frac{1}{2\pi N_q B_q} \sum_{i=1}^{N_q} e^{-\frac{(\bar{b} - \bar{b}_i)^2}{2B_q}}$$

Variable Hotspot Width (VHW):

$$B_q(x_{IP}) = B_{hs} x_{IP}^{\lambda_{hs}}$$

Logarithmic model:

$$B_q(x_{IP}) = b_0 \ln^2 \frac{x_0}{x_{IP}}$$

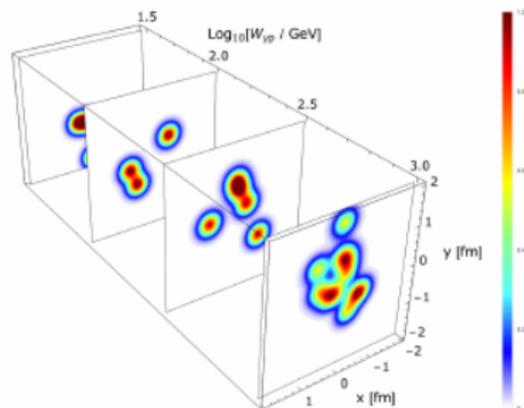
$$r_{\text{rms}} = \sqrt{2(B_{qc} + B_q(x_{IP}))}$$

Modelling x-dependence:

3. Number of Hotspots

$$T_p(b) = \frac{1}{2\pi N_q B_q} \sum_{i=1}^{N_q} e^{-\frac{(\vec{b} - \vec{b}_i)^2}{2B_q}}$$

$$N_q \rightarrow N_q(x_P) = p_0 x_{IP}^{p_1} (1 + p_2 \sqrt{x_{IP}})$$



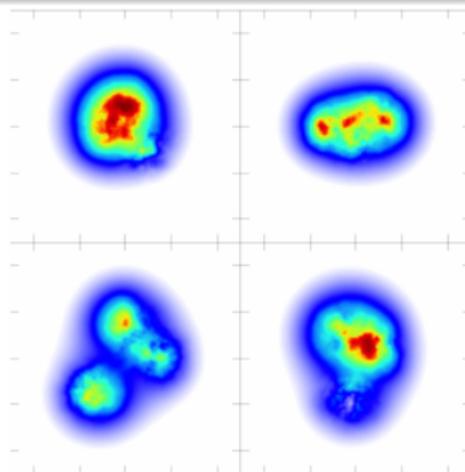
J. Cepila, J. G. Contreras, J. D. Tapia Takaki,
*Energy dependence of dissociative J/ψ
 photoproduction as a signature of gluon saturation at
 the LHC,*
 Phys. Lett. B 766 (2017) 186–191.

$$p_0 = 0.011, p_1 = -0.56, p_2 = 165$$

Going beyond a round proton

Motivation

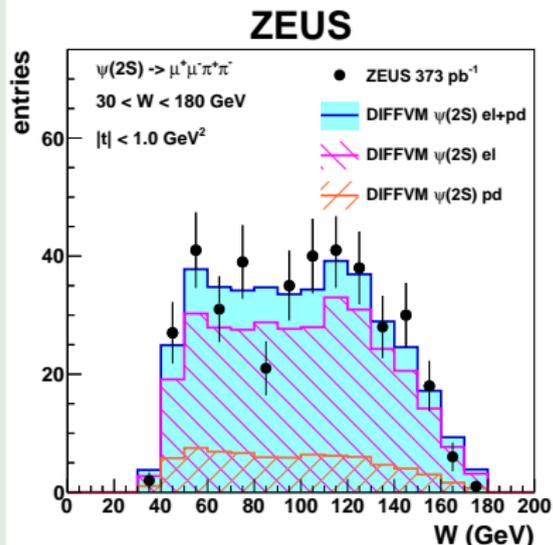
- How does the proton geometry fluctuate event-by-event?
- How accurately can we constrain the proton shape fluctuations, and how do these uncertainties propagate from HERA to e.g. flow@LHC
⇒ Bayesian analysis



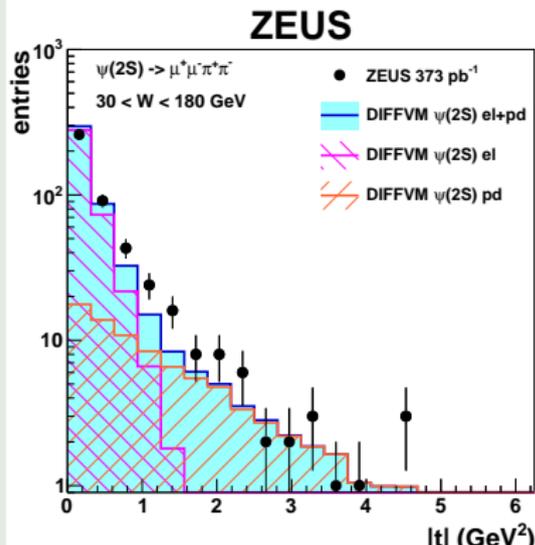
- **More control plots, ...**

4-prongs: W and $|t|$ distributions: $\psi(2S)$ mass window

W : $3.4 < M(\mu^+\mu^-\pi^+\pi^-) < 4.0$ GeV

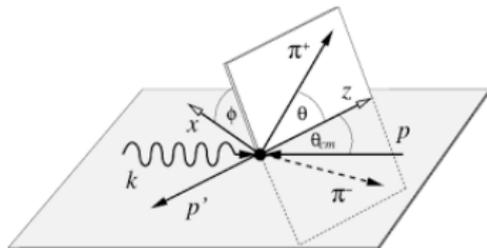
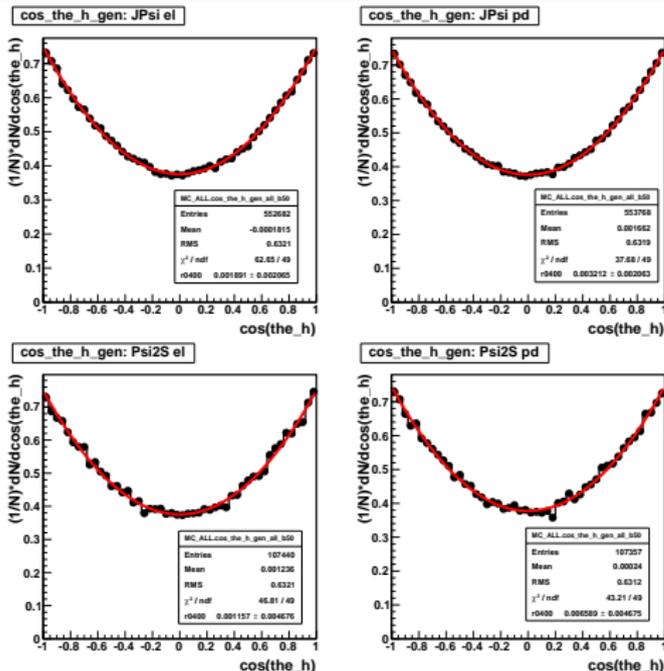


$|t|$: $3.4 < M(\mu^+\mu^-\pi^+\pi^-) < 4.0$ GeV



- proton dissociation dominates for $|t| > 1.0$ GeV²
- proton dissociative fraction: $f_{p,diss} = 0.16 \pm 0.01$ ($|t| < 1.0$ GeV²) from t -spectra fit

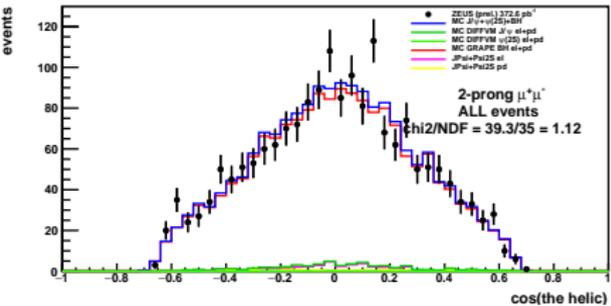
2-prongs: helicity on generator level (before cuts)



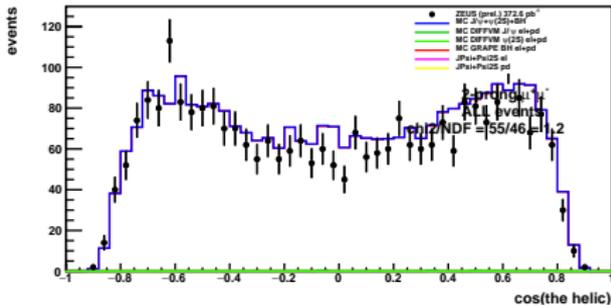
- $\frac{1}{N} \frac{dN}{d\cos\theta_h} = \frac{3}{8} (1 + r_{00}^{04} + (1 - 3r_{00}^{04}) \cos^2\theta_h)$
- for J/ψ and $\psi(2S)$ (el and pd) r_{00}^{04} is 0.0 within errors (as for SCHC)

2-prongs: helicity: $\cos(\theta_h)$

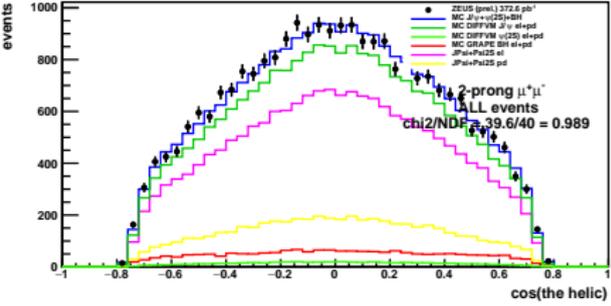
cos_the_h_b50_BH_loM



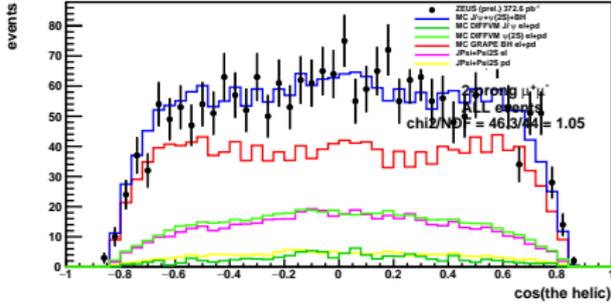
cos_the_h_b50_BH_hiM



cos_the_h_b50_JPSI

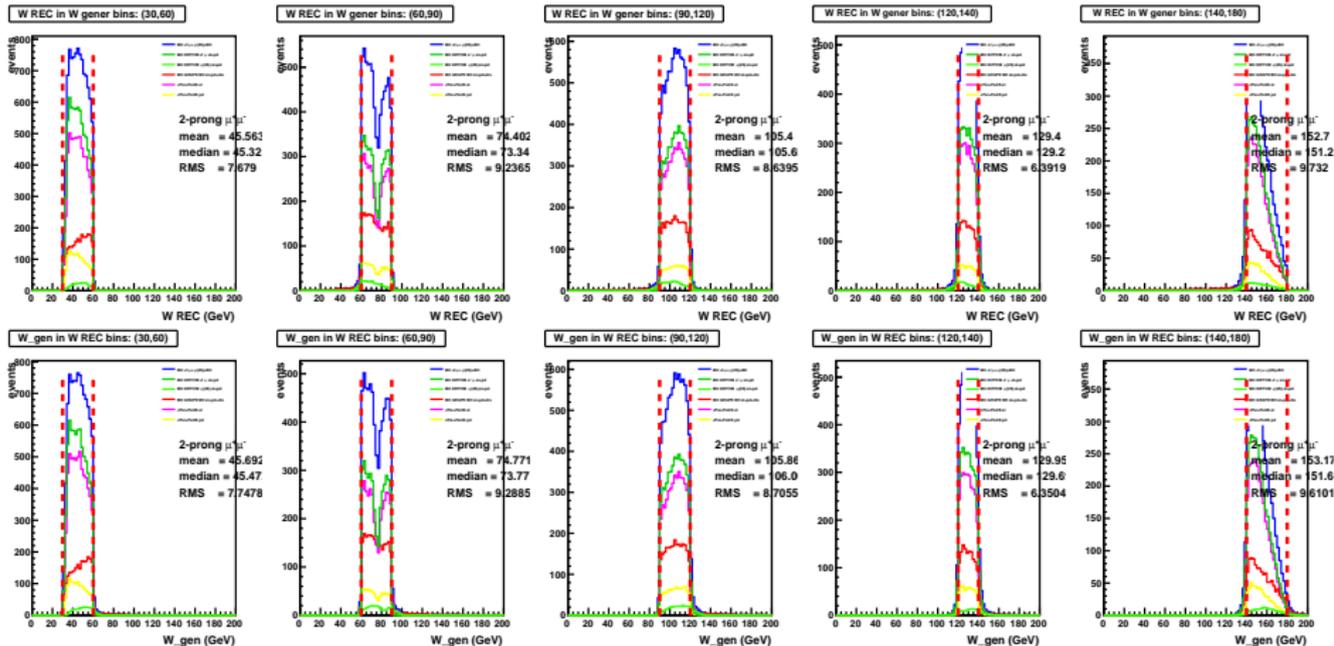


cos_the_h_b50_PSI2S



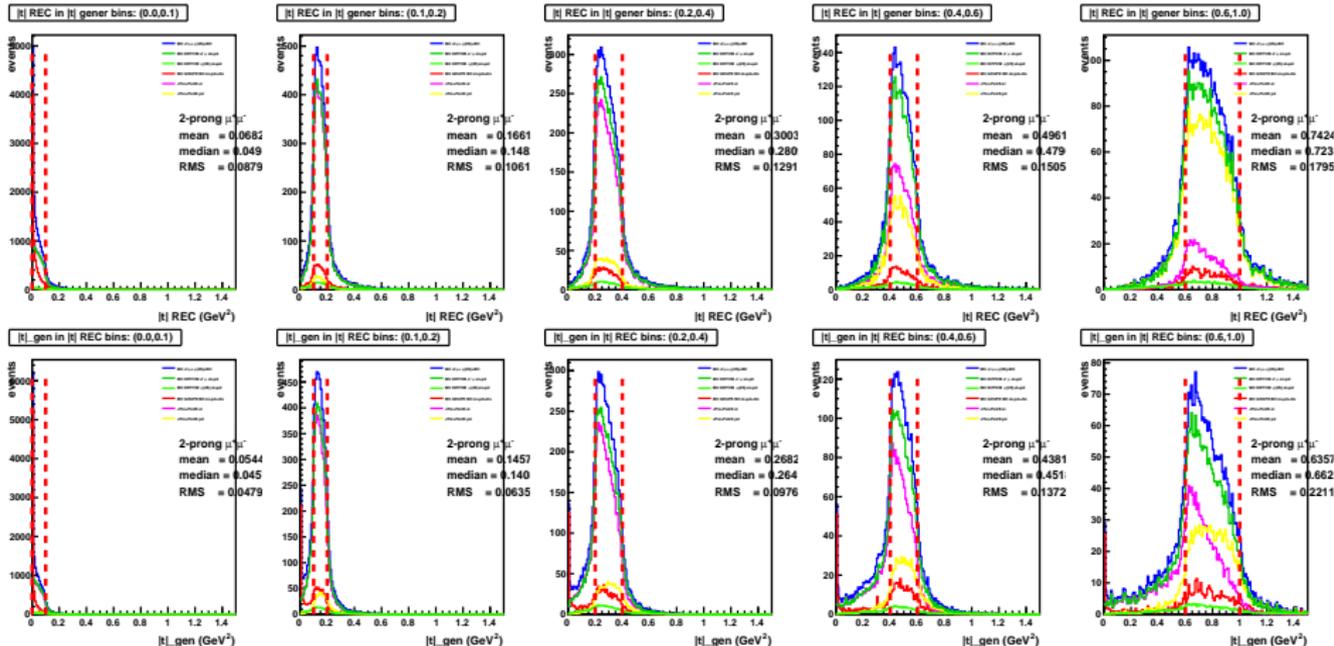
- BH-loM, BH-hiM, J/ψ peak, ψ' peak
- Magenta: elastic contribution, Yellow: p-dissociation, Red: BH
- **SCHC: s-channel helicity is conserved for VM !**

W binning



- 5 W bins ($W1 \div W5$): (30 – 60 – 90 – 120 – 140 – 180) GeV
- almost equidistant : equal statistic, **both dips in $W/2$ bin**
- W_{REC} in W_{GEN} bins (upper row), W_{GEN} in W_{REC} bins (lower row)
- **no migration between bins**

$|t|$ binning



- 5 $|t|$ bins ($t_1 \div t_5$): (0.0 – 0.1 – 0.2 – 0.4 – 0.6 – 1.0) GeV²
- non-equidistant bins : \rightarrow similar statistic for $\sim \exp()$ distribution
- t_{REC} in t_{GEN} bins (upper row), t_{GEN} in t_{REC} bins (lower row)
- some migration to neighbor bins, symmetric, mean value little affected

- **DIFFVM and GRAPE Monte Carlo**

DIFFVM – A Monte Carlo Generator for Diffractive Processes in ep Scattering.

B. List

CERN –EP/OPAL–,
CH–1211 Genève 23, Switzerland
Benno.List@cern.ch

A. Mastroberardino

Calabria University, Physics Dept.,
Cosenza, Italy
mastrobe@vxdesy.desy.de

- soft diffractive processes in the Regge framework and Vector Dominance Model

$$\bullet \frac{d\sigma}{dQ^2} \propto \frac{1}{(1+Q^2/M_Y^2)^{1.5}}$$

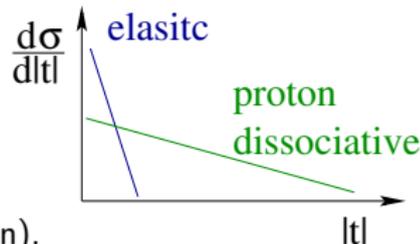
$$\bullet \frac{d\sigma}{d|t|} \propto W_{\gamma p}^{4\epsilon} e^{-b|t|} \quad (4\epsilon = \delta) \text{ (elastic)}$$

$$\bullet \frac{d^2\sigma}{d|t|dM_Y^2} \propto W_{\gamma p}^{4\epsilon} e^{-b'|t|} M_Y^{-\beta} \text{ (p.diss)}$$

$$\bullet \frac{d\sigma}{dM_Y^2} \sim \frac{f(M_Y^2)}{M_Y^{2(1+\epsilon)}} \text{ for } M_Y^2 < 3.6 \text{ GeV}^2 \text{ (} p \text{ resonance region),}$$

$$\frac{d\sigma}{dM_Y^2} \sim \frac{1}{M_Y^{2(1+\epsilon)}} \text{ for } M_Y^2 \geq 3.6 \text{ GeV}^2 \text{ (continuum region)}$$

- assuming SCHC: s-channel helicity conservation



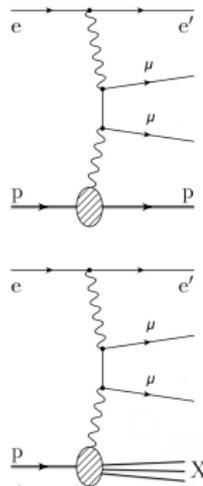
GRAPE-Dilepton (Version 1.1)

A generator for dilepton production in ep collisions

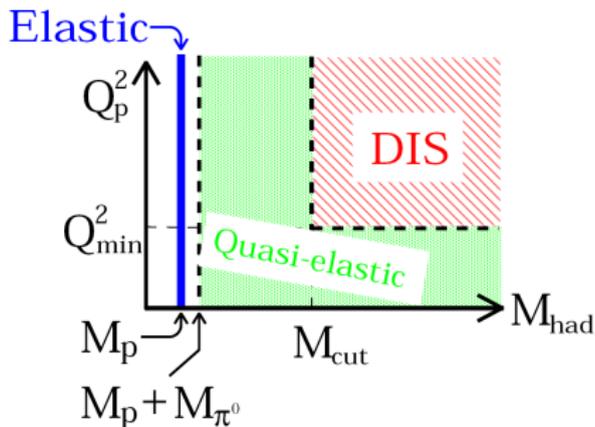
Tetsuo Abe

Department of Physics, University of Tokyo, 7-3-1 Hongo, Bunkyo-ku, Tokyo 113-8654, Japan

- based on the **exact matrix elements** in the electroweak theory at tree level via $\gamma\gamma$, γZ^0 , $Z^0 Z^0$ and via photon internal conversion (QED Compton)
- **Feynman amplitudes** are generated by the automatic calculation system **GRACE**
- **proton vertex** covers the whole kinematical region
- interface to PYTHIA and SOPHIA
→ complete hadronic final state
- covers **elastic, quasi-elastic and DIS processes**



GRAPE generator - simulate QED lepton pair (Bethe-Heitler)



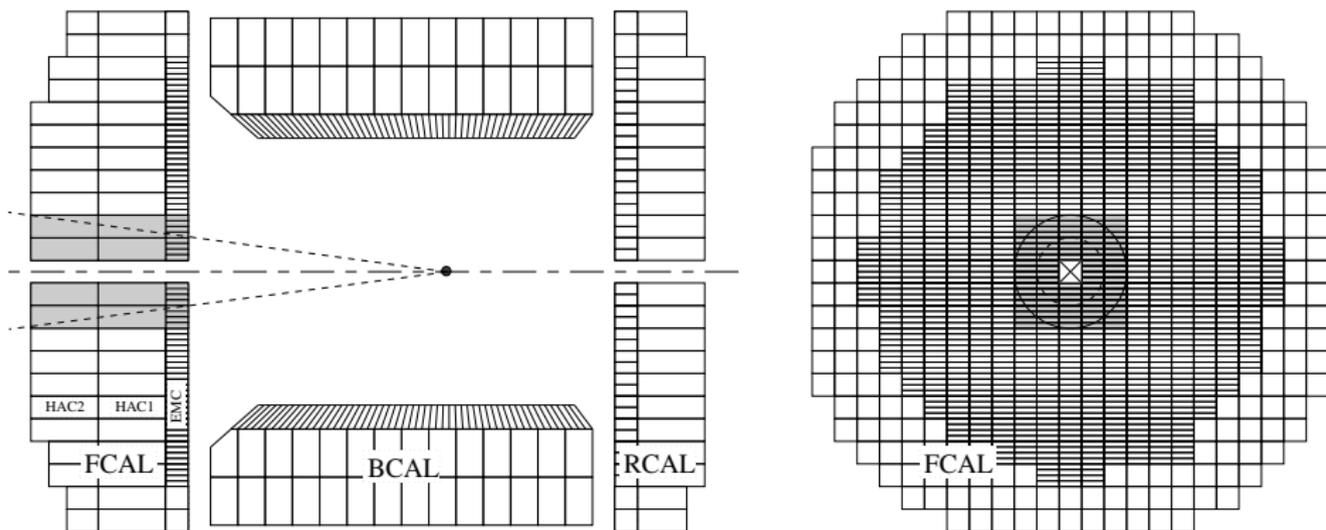
Important for the **shape of the BH $M_{\mu^+\mu^-}$ spectrum** (sidebands)
 and for the **BH t -dependence**: low t - elastic BH, higher t - QEL BH

- **Tuning of DIFFVM Monte Carlo**

- Reweighting of MC sample at generator level
- **|t| dependence**: $\sim \exp(-b|t|)$, generated with $b_{el} = 4.0$, $b_{pd} = 1.0$
reweighted to:
 $b_{el} = 4.6 \pm 0.3$, $b_{pd} = 1.0 \pm 0.1$ (JPSI)
 $b_{el} = 4.3 \pm 0.7$, $b_{pd} = 0.7 \pm 0.2$ (PSI2S)
- shrinkage added by reweighting: $b = b_0 + 4.0\alpha' \log(W/W_0)$;
 $\alpha' = 0.12 \pm 0.04 \text{ GeV}^{-2}$, $W_0 = 90 \text{ GeV}$ (elastic only)
- **W dependence**: $\sigma \sim W^\delta$,
generated with $\delta = 0.88$ for both elastic and p.diss
reweighted to:
 $\delta_{el} = 0.67 \pm 0.10$, $\delta_{pd} = 0.42 \pm 0.15$ (JPSI)
 $\delta_{el} = 1.10 \pm 0.20$, $\delta_{pd} = 0.70 \pm 0.30$ (PSI2S)
- **M_Y dependence**: $\sim \frac{1}{M_Y^\beta}$, generated with $\beta = 2.5$
reweighted to $\beta = 2.4 \pm 0.3$ (both JPSI and PSI2S, p.diss only)
- **all parameters are subject to systematics checks**

- **extracting fractions of proton dissociation**

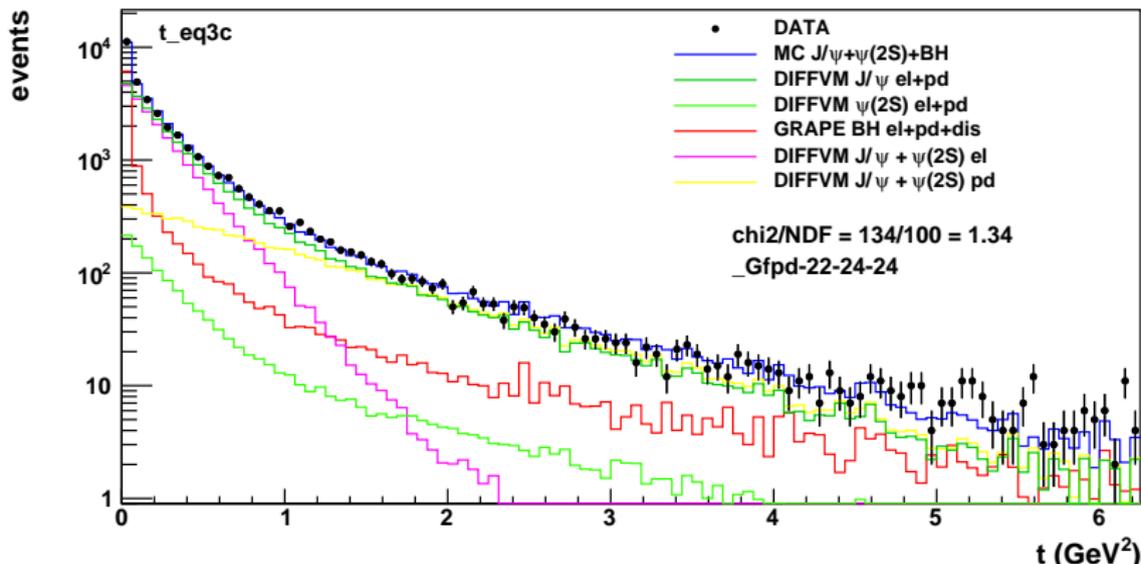
Proton dissociation taggers



- Energy in forward cone to **suppress p.diss events**: $\theta_{max} = 0.12 \text{ rad}$
- using EFO : “Energy Flow Objects” (trackers + CAL info):

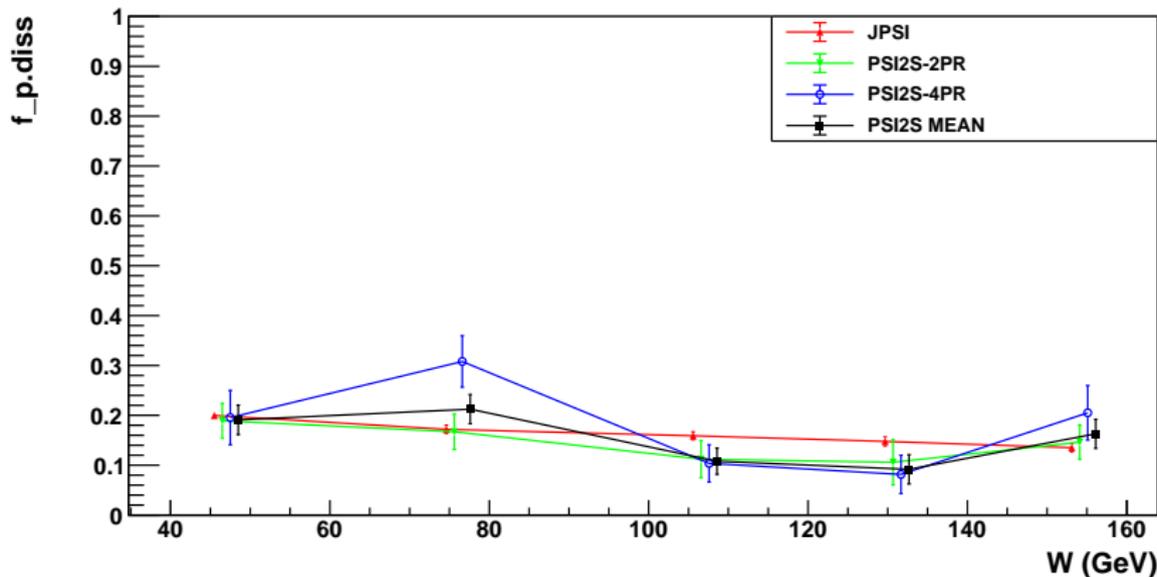
$$\left(\sum_{EFOs} E(\theta_{EFO} < \theta_{max}) \right) < 1 \text{ GeV}$$

2-prongs: $|t|$ distribution: all 2-prong events



- spectra like this are used to evaluate the p.diss fractions (use longer “lever arm” then integrate it up to $|t| = 1.0 \text{ GeV}^2$)
- using root package TFractionalFitter (TFF)
- fitted $f_{p.diss} = 0.17$ and $= 0.16$ (JPSI and PSI2S, BH subtracted)
- p.diss take over elastic around $\sim 1 \text{ GeV}^2$ (yellow and magenta histos)

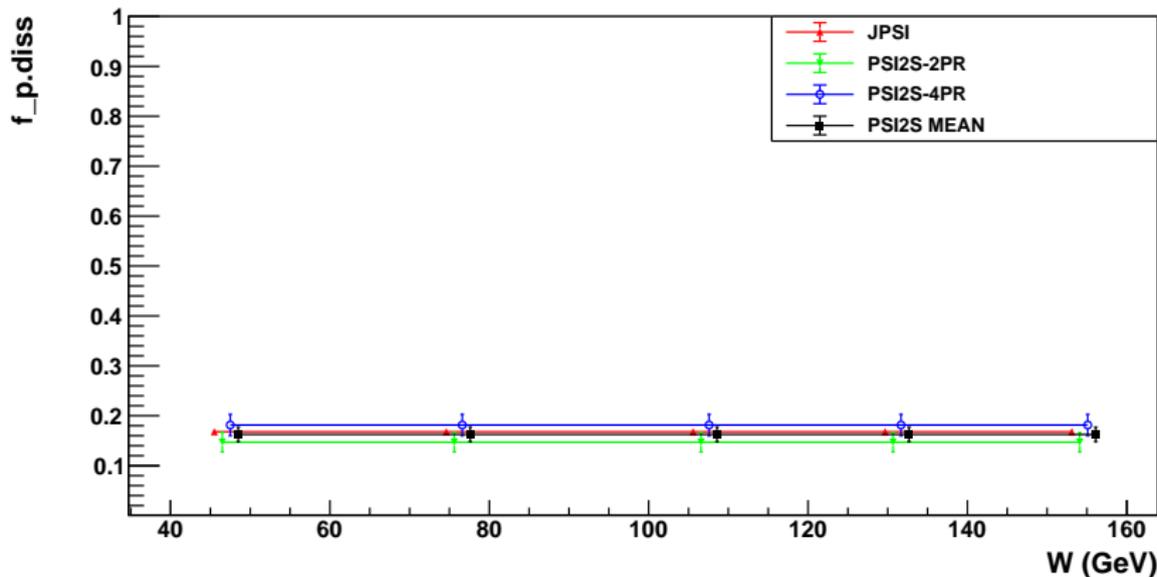
fraction $f_{p,diss}$: JPSI and PSI2S 2PR, 4PR vs. W



- average value $\sim 17\%$ JPSI and $\sim 16\%$ PSI2S (mean)
- compatible results for 2- and 4-prong channels, no W dependence
- **black**: weighted mean for PSI2S 2- and 4-prong
- bigger fluctuations for PSI2S 2- and 4-prongs

$f_{p.diss}$ fractions in W bins (TFF estimator)

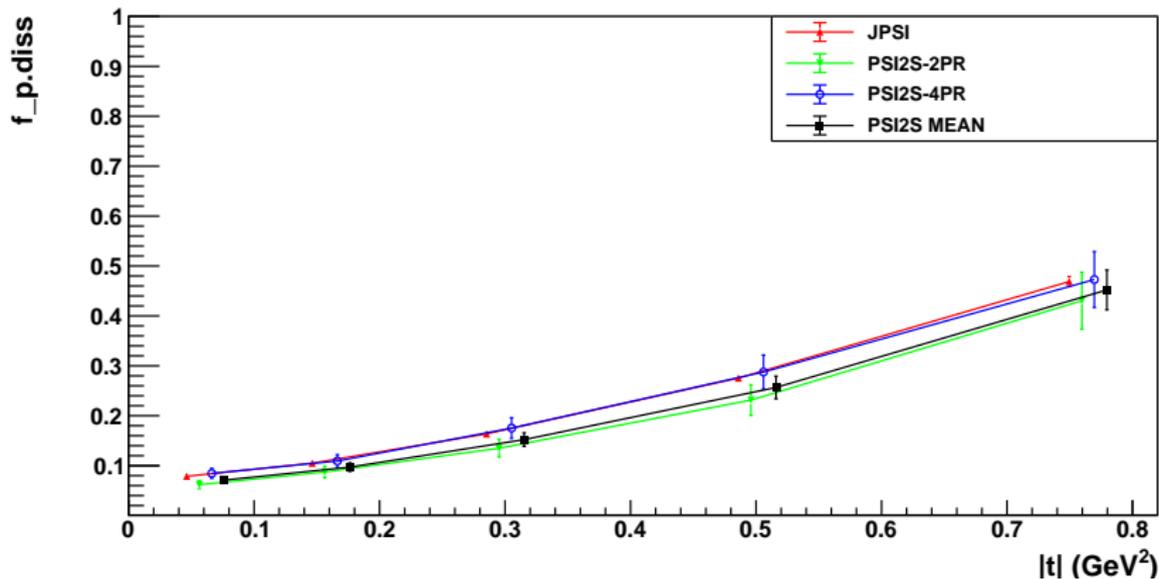
fraction $f_{p.diss}$: JPSI and PSI2S 2PR, 4PR vs. W



- average value $\sim 17\%$ JPSI and $\sim 16\%$ PSI2S (mean)
- **black**: weighted mean for PSI2S 2- and 4-prong (used in analysis)
- **for R analysis: the same mean value is used for all W bins**
- no significant impact on final ratio R ($f_{p.diss}$ fractions cancels out)

$f_{p,diss}$ fractions in $|t|$ bins (TFF estimator)

fraction $f_{p,diss}$: JPSI and PSI2S 2PR, 4PR vs. $|t|$



- compatible results for 2- and 4-prong channels
- **black**: weighted mean for PSI2S 2- and 4-prong (used in analysis)
- negligible effect on final R analysis ($f_{p,diss}$ fractions cancels out)
- bigger impact on systematics for large $|t|$ due to the b -slope variation !

- **Modeling of nucleon resonance states**
- (low M_Y proton dissociation)

- $\frac{d\sigma}{dM_Y^2} \sim \frac{1}{M_Y^{2(1+\epsilon)}}$ for $M_Y^2 \geq 3.6 \text{ GeV}^2$ (continuum region)
- $\frac{d\sigma}{dM_Y^2} \sim \frac{f(M_Y^2)}{M_Y^{2(1+\epsilon)}}$ for $M_Y^2 < 3.6 \text{ GeV}^2$ (p resonance region)
- $f(M_Y^2)$ from the **fit the the p.diss cross section on deuterium**:
 $pD \rightarrow YD$ (Phys. Rep. **101** (3) (1983), 169)
- for $M_Y < 1.9 \text{ GeV}$ several resonances are included
(Pomeron carries quantum numbers of the vacuum ($l=0, G = P = C = +$)
only N^{*+} states with $J^P = \frac{1}{2}^+, \frac{3}{2}^-, \frac{5}{2}^-, \dots$)
- $N^{*+} = N(1440), N(1520), N(1680), N(1700)$
- N^{*+} decays into: $N\pi, \Delta\pi, N\rho, N\pi\pi$ included (BR from PGD 1992)
- N^{*+} decays isotropically in their rest frame
- dissociation in the continuum state carried by JETSET
(splitting proton into $q - qq$ system, q couples to \mathbb{P} , leaving qq spectator)

- $d\sigma \sim L_{\mu\nu} W^{\mu\nu}$

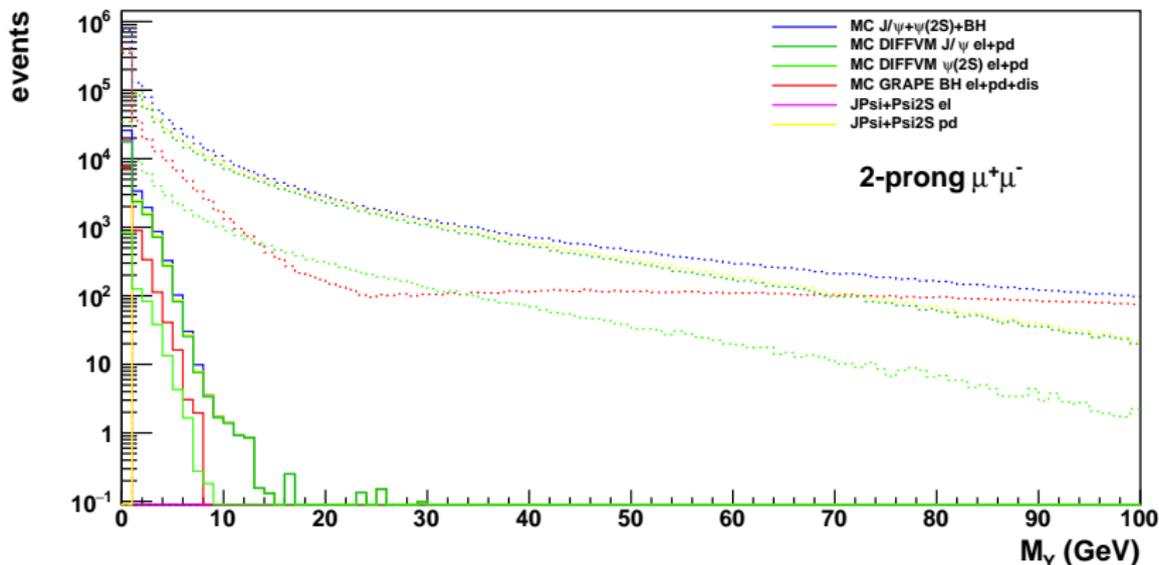
- hadron tensor:

$$W^{\mu\nu} = W_1 \left(-g^{\mu\nu} + \frac{q^\mu q^\nu}{q^2} \right) + W_2 \frac{1}{M_p^2} \left(p_P^\mu - \frac{p_P \cdot q}{q^2} q^\mu \right) \left(p_P^\nu - \frac{p_P \cdot q}{q^2} q^\nu \right)$$

- $W_{1,2}(Q_P^2, M_{had})$ are proton electromagnetic structure functions
- for $M_{had} < 2$ GeV $W_{1,2}$ parameterized by Brasse at al. (Nucl. Phys. **B 110** (1976) 413.) (resonance region)
- for $M_{had} > 2$ GeV $W_{1,2}$ parameterized by ALLM97 (hep-ph/9712415) (continuum)
- both parameterizations from **fits to experimental total $\gamma^* p$ cross sections**
- exclusive hadronic final state generated by SOPHIA
- (plus DIS di-leptons diagrams, in the framework of QPM, using PDF's)

MC generator level: M_Y before and after selection cuts

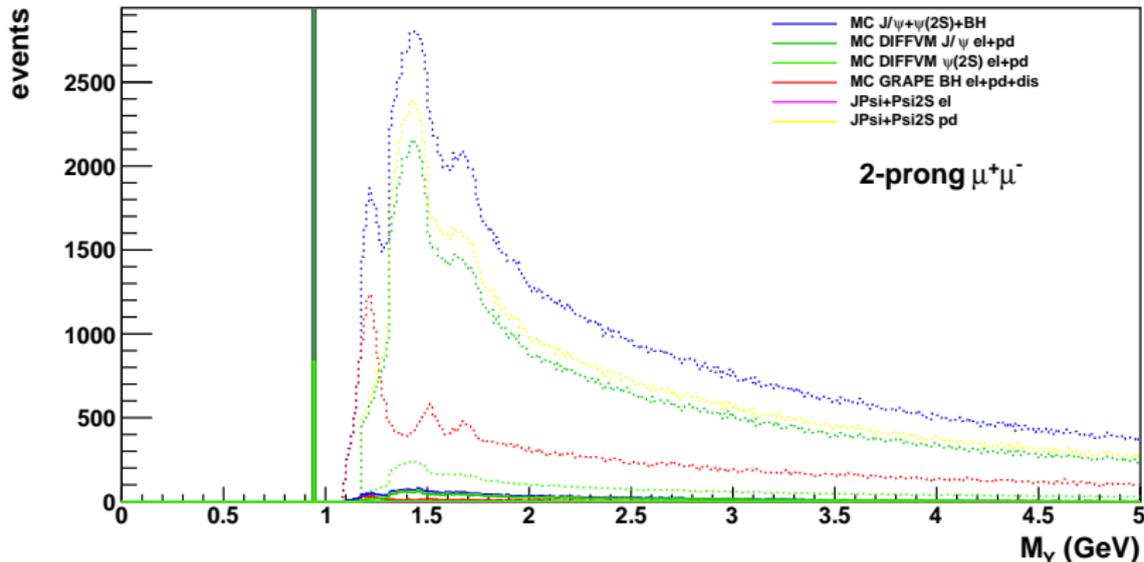
M_Y gener before and after cuts



- M_Y at generator level (not measured quantity ! \rightarrow lost in beam-pipe)
- before and after selection cuts
- GRAPE (BH) does include DIS scattering \rightarrow rise of xsec. for large M_Y
- DIFFVM in DIS mode generates only **electroproduction** (with proton dissociation, "rapidity gap events") \rightarrow this is OK

MC generator level: zoom at low $M_Y < 5$ GeV (lin scale)

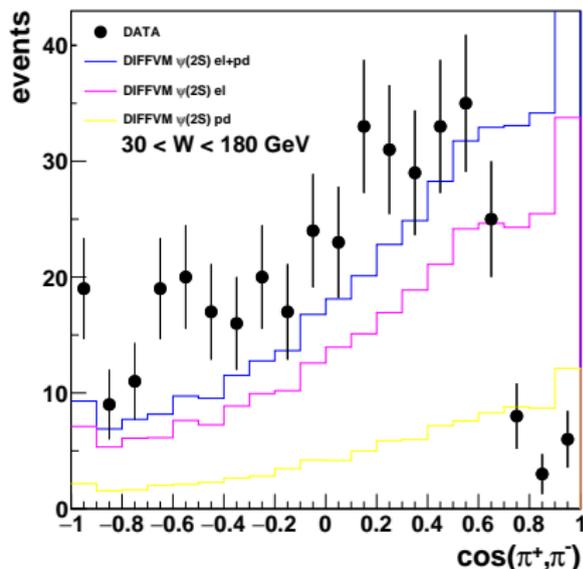
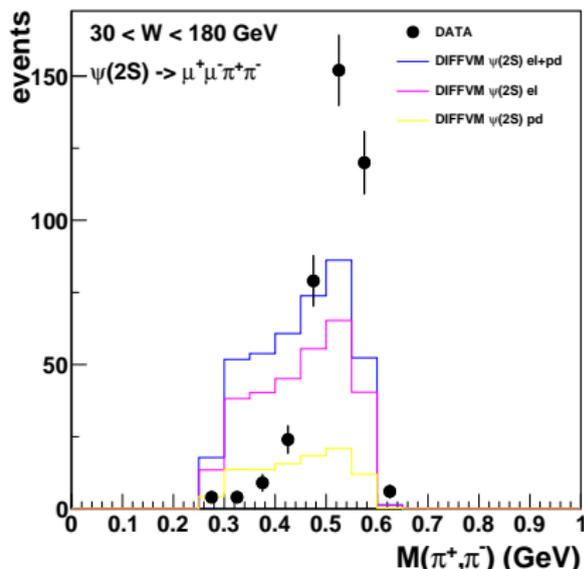
M_Y gener before and after cuts



- different structure of nucleon resonances between **GRAPE** and **DIFFVM** (!?)
- which is right ?
- how much it is important for MC based p.diss BG subtraction ?

- Pions phase space reweighting

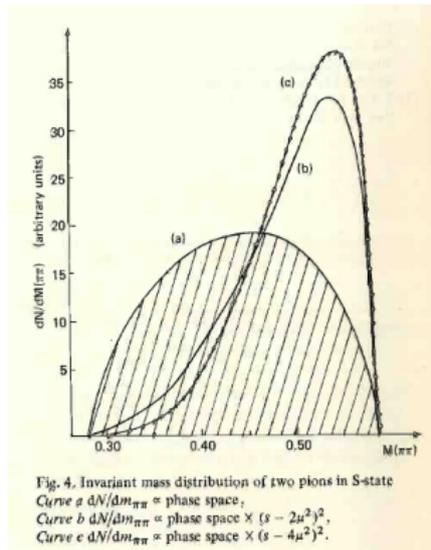
4-PRONGS: $M(\pi^-, \pi^+)$, $\cos(\pi^-, \pi^+)$



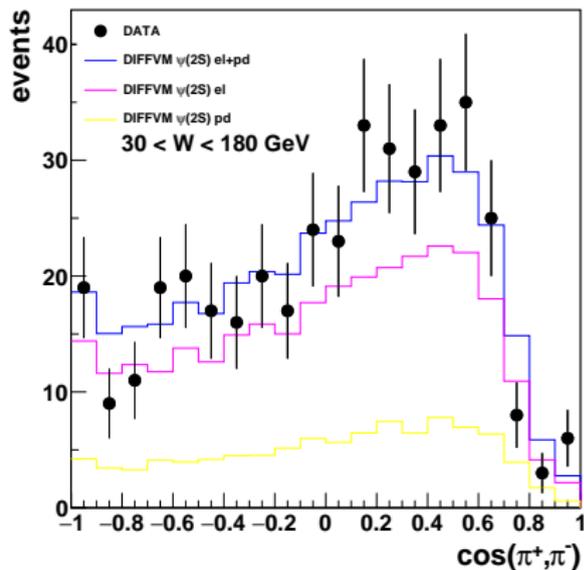
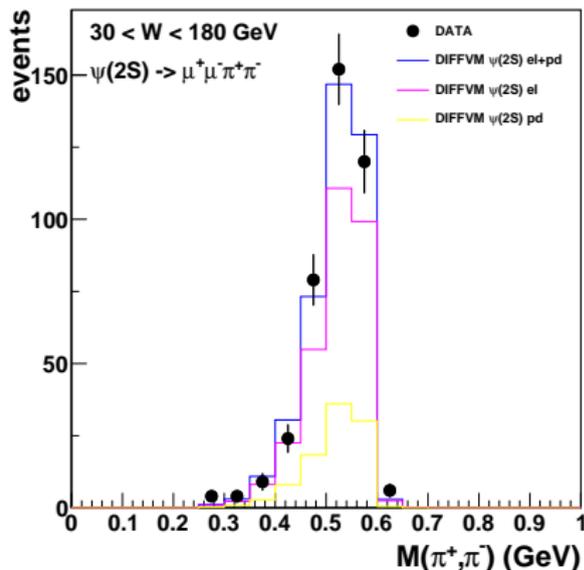
- $\psi' \rightarrow J/\psi + \pi^+ \pi^-$
- $M(\pi^-, \pi^+)$, $\cos(\pi^-, \pi^+)$
- DIFFVM MC **before** pions phase space reweighting

Pions phase space reweighting (DIFFVM 4-prongs)

- $weight = (M(\pi^-, \pi^+)^2 - 4.0 * M_\pi^2)^2$
- ref: Phys_Lett_B61_1976_183.pdf
- final $\pi^+\pi^-$ interaction is not in pure S-state
- → for the impact of this correction see next 2 pages



4-PRONGS: $M(\pi^-, \pi^+)$, $\cos(\pi^-, \pi^+)$



- $\psi' \rightarrow J/\psi + \pi^+ \pi^-$
- $M(\pi^-, \pi^+)$, $\cos(\pi^-, \pi^+)$
- DIFFVM MC **after** pions phase space reweighting